A THEORETICAL AND EXPERIMENTAL INVESTIGATION OF SOME ASPECTS OF THE HILSCH TUBE

by

WILLIAM L. SLAGER

Submitted in Partial Fulfillment
of the Requirements for the
Degree of Bachelor of Science
at the
MASSACHUSETTS INSTITUTE OF TECHNOLOGY
June, 1959

Signature of Author

Dept. of Mechanical Engineering, May 25, 1959

Certified by

Thesis Supervisor

Accepted by

Chairman, Departmental committee on theses

32 Hereford Street
Boston 15, Massachusetts
May 25,1959

Professor Alvin Sloane
Secretary of the Faculty
Massachusetts Institute of Technology
Cambridge 39, Massachusetts

Dear Sir,

In accordance with the requirements of the Massachusetts Institute of Technology, I hearby submit my thesis entitled "A Theoritical and Experimental Investigation of Some Aspects of the Hilsch Tube", in partial fulfillment of the requirements for the degree of Bachelor of Science in Mechanical Engineering.

Sincerely yours,

William L. Slager

Acknowledgement

The major part of this thesis was carried out under the guidance of Professor J. L. Smith , of the M. I. T. Mechanical Engineering Department.

His knowledge and previous experience, gained in working with cyclone seperators and allied equipment using the vortex principle, were invaluable and continually served to stimulate my interest.

I would also like to thank Mr. C. B. Dolber and especially Mr. C. W. Christiansen, who helped me immensely in the construction of the experimental equipment.

Abstract

A theoretical analysis of the internal operation of the Hilsch tube or vortex refrigerator was carried out. The analysis assumed that a major factor influencing the performance of the device was the frictional effects of wall shear forces inside the refrigerator. The type of solution obtained by assuming an incompressible working fluid has been visually observed in previous experiments where this assumption was valid.

A method of obtaining a solution when a compressible fluid is used is outlined.

A vortex chamber attachment having as its purpose the pre-acceleration of the working fluid before entrance into the Hilsch tube was analyzed and a theoretical design criterion was obtained.

The attachment was tested experimentally and was found to deliver the same flow rate of refrigerated fluid 20^{0} F colder then a similar vortex tube with no such device, while maintaining the initial inlet pressure.

The effect of placing various circular flow restricting weirs at the hot air exit of the refrigerator was observed experimentally to have an apparently

detrimental effect.on the performance of the Hilsch tube.

Table of Contents

Introduction

Historical

The early history of the Hilsch tube may be best summarized by the following excerpt from Scientific American.(1)

"Shortly after the end of World War II, word came to the U.S. that the Germans had developed a remarkably simple device with which one could reach temperatures as low as the freezing point of mercury. The device was said to consist only of an air compressor and three pipes. The details of construction were not available, but it was reported that the device had in effect realized Maxwell's demon, a fanciful means of seperating heat from cold without work."

"...When physicists heard that the Germans had developed a device which could achieve low temperatures they were intrigued though obviously skeptical. One physicist Robert M. Milton, investigated the matter first hand for the U.S. Navy."

"Milton discovered that the device was most ingenious, though not quite as miraculous as had been rumored. It consisted of a T-shaped assembly of pipe joined by a novel fitting (Fig.1). When compressed air is admitted to the leg of the T, hot air comes out

of one arm of the T and cold air out of the other arm! Obviously however, work must be done to compress the air."

"The origin of the device is obscure. The principle is said to have been discovered by a Frenchman who left some early experimental models in the path of the German Army when France was occupied. These were turned over to a German physicist named Rudolf Hilsch who was working on low temperature devices for the German war effort. Hilsch made improvements on the Frenchman's design but found that it was no more efficient then conventional methods of refrigeration in achieving fairly low temperatures, subsequently the device became known as the Hilsch tube."

Hilsch's Investigation

After the war Hilsch published a paper,"The Use of the Expansion of Gases in a Centrifugal Field as a Cooling Process" (2) in which he presented the results of his experimentation with the device(Fig. 1). He found that by introducing compressed air into the pipe containing his ingenious spiral mechanism at 68 ^{0}F , he could obtain by suitably varying the significent parameters, a maximum cold air temperature of approximately -60 ^{0}F and a maximum hot air temperature of approximately 390 ^{0}F although not simultaneously.

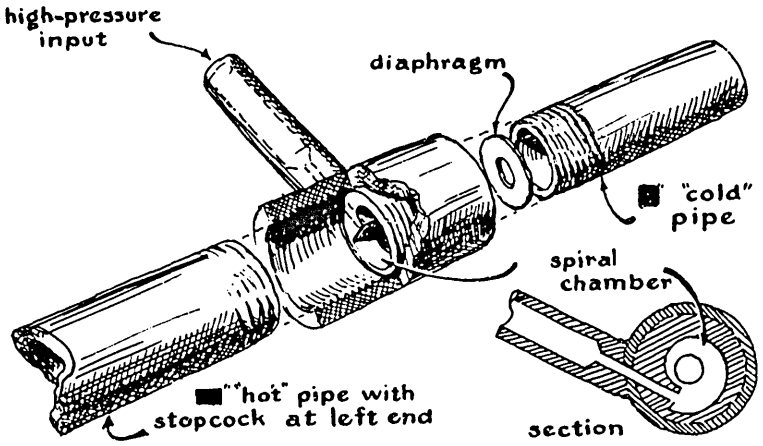

Cutaway views of the Hilsch tube

Fig. 1

The parameters which influenced the temperatures of the gas flows he found to be; 1) the temperature,, pressure, and flow rate of the compressed air into the pipe; 2) the ratio of the diameters of the hot pipe, cold air diaphragm and compressed air inlet nozzle; 3) the ratio of distribution of flow in both directions, which he varied by setting a valve on the end of the hot pipe and; 5) the external pressure outside of the device. The length of the cold pipe had no effect in the tube's performance.

He also observed that by increasing the size of the hot pipe, inlet nozzle and diaphragm in geometric proportion, lower values of cold temperatures were obtained at the same inlet pressure and the thermodynamic efficiency of the device increased.

In spite of the impressive performance of the Hilsch tube, it's efficiency was found to be low. The best efficiency Hilsch could obtain with the larger size pipe was 20%.

Various Theories About the Hilsch Tube

Hilsch successfully recorded the external data which could be obtained from the device, but presented only a qualitative picture of the phenomenon occuring inside the tube. No one has yet adequately analyzed the internal operation of this device mathematically,

and there seems to be some disagreement about the significant aerodynamic mechanism which is responsible for the temperature seperation.

In the usual experimental setup (Fig. 2), the air, which is introduced by a nozzle or nozzles tangentially placed on the tube wall, spirals down the hot tube. The flow through the cold air diaphragm is regulated by changing the back pressure in the hot pipe with a valve attached at it's end.

Experimentally it is found that the motion of the air near the tube walls resembles that of an irrotational or free vortex and the motion of the air in the center of the pipe is a rotational or forced vortex.

A typical tangential velocity distribution obtained in the Hilsch tube is shown in Fig. 2, illustrating the nature of the transition from a free to a forced vortex within the tube.

According to one theory, as the tangential velocity of the outer irrotational flow increases with decreasing radius, viscous effects become important and the shear forces between the air particles act to reduce the velocity of the inner layers of air such that near the centerline of the pipe there is a core of air rotating as a solid body. During this process the inner layers surrender part of their kinetic energy to the layers near the wall and subsequently some of this cold core

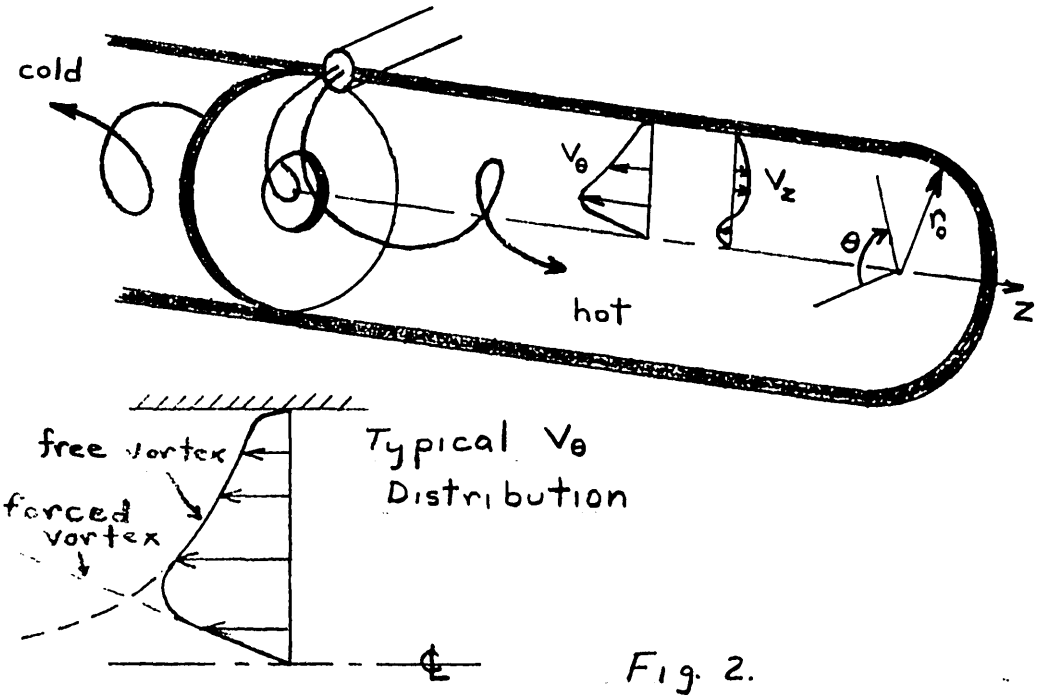
cold
hot
V_θ
V_z
r_0
θ
z
free vortex
forced vortex
Typical V_θ Distribution
$\mathcal{L}$

Fig. 2.

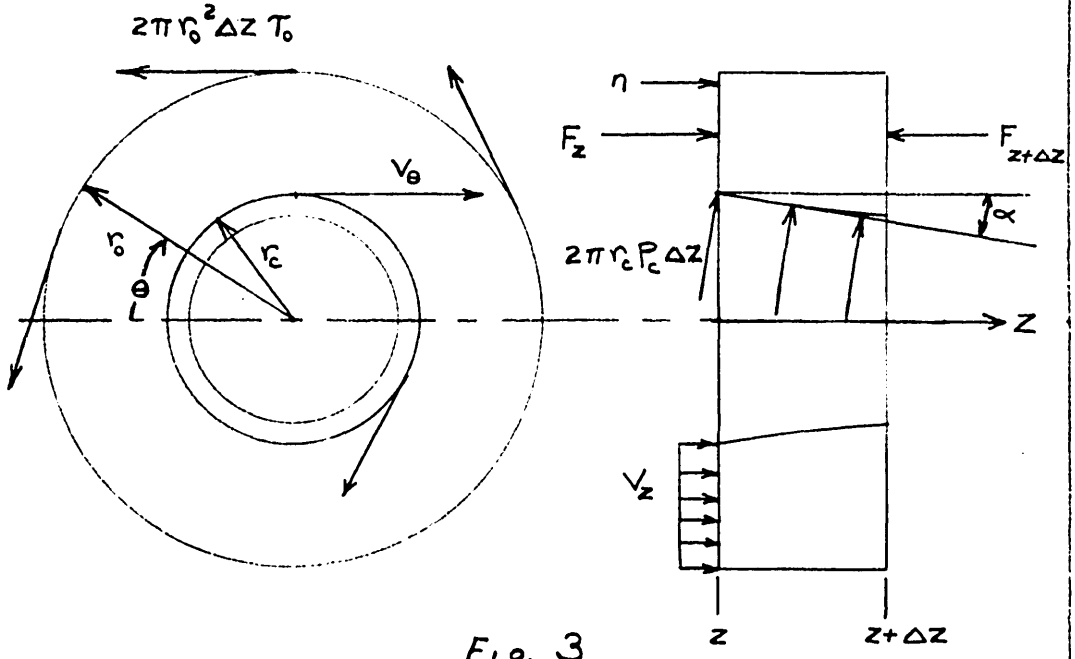
$2\pi r_0^2 \Delta z\, \tau_0$
V_θ
r_0
r_c
θ
$\mathcal{L}$
n
F_z
$F_{z+\Delta z}$
α
$2\pi r_c P_c \Delta z$
z
V_z
z
$z+\Delta z$

Fig. 3

is forced out the cold air diaphrgm by pressure forces.

Another theory contends that near the wall the outer layers of the irrotational flow are slowed by boundary-layer stresses to a small velocity. The intermediate layers with a higher rotational velocity transfer some of their energy to the outer layers in an 'attempt' to speed them up. As the flow progresses down the tube, the overall tangential velocity profiles decrease due to the accumulated frictional effect. Again the overall result is to create a core of cold air near the center of the pipe and a hot one near the wall. (3)

Another mechanism of heat transfer theorized to be present within the tube again involves the boundary-layer. Molecules of air entering the boundary layer on the wall are slowed to a small velocity. Because of their lack of angular momentum these particles are unstable with respect to the rest of the centrifugal field. They tend to pile up into a packet, which is eventually swept away from the wall and moves to a more stable position near the center of the pipe, where the angular momentum is also small. The net result of the process is the accumalation of low energy molecules in the center of the pipe and high energy ones near the wall. (4)

(4)

Difficulty of a Direct Solution

It is quite possible that all three of the previously mentioned theories figure into an adequate solution of the Hilsch tube. There seems to be agreement that in the phenomenon viscous forces, wall shear stresses and compressibility effects are not neglible and occur in at least two dimensions.

The only mathematical tool which can handle these effects simultaneously is the Navier-Stokes equations coupled with the energy equations for a Newtonian fluid. However, these equations become complex in the extreme when all the above effects are considered, and at present only special cases of these equations have been solved by neglecting one or more of the above effects.

Even if a solution were discovered it might still only be approximate because of the high Reynold's numbers and correspondingly turbulent flow within the tube.

Purpose of Thesis

One of the objects of this thesis was to study the second of the aforementioned theories. By considering wall shear forces as a major factor in the performance of the Hilsch tube, it was hoped that the results obtained would clarify some aspects of the internal operation of this device.

Another aim was to try out experimentally a vortex chamber pre-accelerating device which seemed promising when previous data was considered. This device would increase the inlet air tangential velocity in a manner similar to a converging-diverging nozzle, but had the advantage of introducing the flow evenly at the perimeter of the hot pipe, while using the same inlet pressure as a tube with no such device. It was hoped that such a device might increase the efficiency of the Hilsch tube.

Theoretical Analysis

List of symbols not otherwise defined in text

f - pipe friction factor - dimensionless

F - force - lb_f

H - Bernoulli constant or 'total head' - ft.

k - dimensionless ratio of specific heats of air - 1.40

n - unit normal vector

P - fluid pressure - lb_f/ in^2

r - radial distance - inches

R - gas constant for air - 53.35 $ft\text{-}lb_f/ lb_m\ ^oF$

T - farenheit temperature

V - velocity - ft/ sec

w - fluid flow rate - $lb_m/$ sec.

z - axial distance - feet

Greek symbols

ϵ - ratio of cold fluid flow to total flow

ρ - fluid density - lb_m/ ft^3

τ - wall shear stress - lb_f/ in^2

Subscripts

0 - applies to wall of hot pipe (Fig. 3)

1 - applies to outer radius of vortex pre-accelerator (Fig. 8)

c - pertains to boundary between rotational and

and irrotational flow (Fig. 3)

h - hot fluid

r - radial direction

s - stagnation conditions

w - inside radius of weir

z - axial direction

θ - tangential direction

* - refers to points where the Mach number is one.

Part I

Derivation of the Flow Pattern of the Hot Fluid

This study presents the theoretical results obtained assuming that an important factor in the operation of the Hilsch tube is the frictional effects of wall shear stresses. It is limited to an incompressible fluid and deals specifically with the hot fluid inside the pipe.

The following assumptions were made:

#1 The flow pattern was broken up into two regions, an outer irrotational layer and an inner rotational core, seperated by a boundary along which the pressure in the fluid was assumed to be constant. It was furthur assumed that along the boundary the radial velocity was zero, so that no fluid crossed the boundary.

#2 The fluid density was taken to be constant.

#3 All shear stresses in the fluid were neglected, except those at the wall which were taken to be

$$\tau = \frac{f\rho V_\theta^2}{8}. \quad (5)$$

#4 The tangential velocity was assumed to be much greater then either the radial or axial velocities.

#5 This led to the assumption that the pressure gradient in the radial direction is given by

$$\frac{\partial P}{\partial r} = \rho \frac{V_\theta^2}{r}.$$

#6 The form of the tangential velocity distribution was taken as $V_\theta = \frac{C(z)}{r}$ where C(z) was a function to be determined.

#7 At any given cross section of the hot pipe, the axial velocity in the outer core was assumed to have a constant value given by the continuity equation.

#8 The fluid flow was assumed to be steady and the pipe walls adiabatic.

Figure 3 shows the nature of some of these assumptions and illustrates an element of the flow within the hot pipe.

With the above assumptions the continuity, linear and angular momentum equations may now be applied by utilizing the integral method, and yield a solution for the flow pattern in the outer layers of hot fluid.

The continuity equation is

1a) $$w_h = \int_{\text{control surface}} (\vec{V}\cdot\vec{n})\, dA \quad . \qquad (6)$$

Taking a small cross section of the flow at z having a width of Δz (Fig. 3), then at z the mass flow into the element is

1b) $$w_{in} = \int_{r_o}^{r_c} \rho\, V_z(-2\pi r\, dr) \quad .$$

At $z + \Delta z$ the mass flow out of the element is

$$w_{out} = \int_{r_o}^{r_c} \rho\, V_z(-2\pi r\, dr) + \frac{d}{dz}\left[\int_{r_o}^{r_c} \rho\, V_z(-2\pi r\, dr)\right] \Delta z.$$

Then

$$w_{out} - w_{in} = 0 = \frac{d}{dz} \int_{r_o}^{r_c} \rho V_z (-2\pi r \, dr) \ .$$

Upon integration, since V_z is constant we obtain

1c) $$w_h = \rho V_z (\pi r_o^2 - \pi r_c^2) \ .$$

Differentiating equation 1c, we obtain another equation which will be useful later,

$$\rho (\pi r_o^2 - \pi r_c^2) \frac{dV_z}{dz} = 2\pi r_c V_z \frac{dr_c}{dz} \ ,$$

inserting equation 1c into the left hand side of the above equation and simplifing , we have finally,

1d) $$\frac{dV_z}{dz} = \frac{2\pi r_c w_h}{\rho (\pi r_o^2 - \pi r_c^2)^2} \frac{dr_c}{dz} \ .$$

The angular momentum equation is for steady flow,

2a) $$\Sigma \vec{F} \times \vec{r} = \int_{out} \rho (\vec{V}_\theta \times \vec{r})(\vec{V} \cdot \vec{n}) \, dA - \int_{in} \rho (\vec{V}_\theta \times \vec{r})(\vec{V} \cdot \vec{n}) \, dA \ . \quad (6)$$

The torque acting on the element in Fig. 3 is

$$\Sigma \vec{F} \times \vec{r} = 2\pi r_o \Delta z (\tau_o \times r_o) = -2\pi r_o^2 \Delta z \tau_o \ .$$

At z the integral

$$\int_{in} \rho (\vec{V}_\theta \times \vec{r})(\vec{V} \cdot \vec{n}) \, dA = \int_{r_o}^{r_c} \rho V_\theta r V_z \ (-2\pi r \, dr)$$

and is directed in the positive z direction.

At $z + \Delta z$

$$\int_{out} \rho (\vec{V}_\theta \times \vec{r})(\vec{V} \cdot \vec{n}) \, dA = \int_{r_o}^{r_c} \rho V_\theta r V_z \cdot (-2\pi r \, dr) + \frac{d}{dz} \left[\int_{r_o}^{r_c} \rho V_\theta r V_z \ (-2\pi r \, dr) \right] \Delta z .$$

Inserting these expressions into the angular momentum equation 2a and substituting in assumption #6 for V_θ, we arrive at

2b) $$2\pi r_o^2 \tau_o = - \frac{d}{dz}\left[\int_{r_o}^{r_c} \rho\, C(z)\, V_z\, (2\pi r\, dr).\right]$$

Removing C(z) from beneath the integral sign but not outside the brackets, the remaining integral in eq. 2b is equal to the flow rate . Using eq. 1b we find

2c) $$2\pi r_o^2 \tau_o = - w_h \frac{dC(z)}{dz} \quad .$$

Since the Reynolds number in a typical Hilsch tube has a large value of approximately $5 \cdot 10^6$ or greater, we will make the additional assumption that the friction factor f may be taken as constant. Then

3a) $$\tau_o = \frac{f}{8} \rho V_\theta^2 = \frac{f \rho C(z)^2}{8 r_o^2} \quad .$$

Inserting this expression into the angular momentum equation (2c) we have

3b) $$\frac{dC(z)}{dz} = - \frac{\pi f \rho C(z)^2}{4 w_h} \quad .$$

Integrating the above equation and choosing the initial condition at z = 0 , $C(z) = C_o = \frac{V_{\text{inlet nozzle}}}{r_o}$ we obtain

3c) $$C(z) = \frac{C_o}{1 + \frac{\pi f \rho C_o}{4 w_h} z} \quad .$$

Applying the linear momentum equation in the z direction, which is

$$4a)\quad \Sigma \vec{F}_z = \int_{out} \rho \vec{V}_z (\vec{V}\cdot\vec{n})\, dA - \int_{in} \rho \vec{V}_z (\vec{V}\cdot\vec{n})\, dA. \qquad (6)$$

Then at z

$$\vec{F}_z = \int_{r_o}^{r_c} \vec{P}\, (-2\pi r\, dr)\ ,$$

acting in the positive z direction.

At $z + \Delta z$

$$\vec{F}_{z+\Delta z} = \int_{r_o}^{r_c} \vec{P}\, (-2\pi r\, dr) + \frac{d}{dz}\left[\int_{r_o}^{r_c} \vec{P}\, (-2\pi r\, dr)\right]\Delta z$$

acting in the negative z direction.

The pressure forces exerted along the core boundary in the positive z direction are

$$\vec{F}_c = 2\pi r_c \Delta z\, \vec{P}_c \sin\alpha$$
$$2\pi r_c \Delta z\, \vec{P}_c \tan\alpha$$
$$-2\pi r_c \Delta z\, \vec{P}_c \frac{dr_c}{dz}\ ,$$

since $\frac{dr_c}{dz}$ is negative. Therefore

$$\Sigma \vec{F} = -2\pi r_c \Delta z\, \vec{P}_c \frac{dr_c}{dz} - \frac{d}{dz}\left[\int_{r_o}^{r_c} \vec{P}\, (-2\pi r\, dr)\right]\Delta z\ .$$

At z the momemtum integral is

$$\int_{in} \rho \vec{V}_z (\vec{V}\cdot\vec{n})\, dA = \int_{r_o}^{r_c} \rho \vec{V}_z^2 (-2\pi r\, dr)\ ,$$

and at $z + \Delta z$ the integral is

$$\int_{out} \rho V_z(\vec{V}\cdot\vec{n})\, dA = \int_{r_o}^{r_c} \rho V_z^2\, (-2\pi r\, dr) + \frac{d}{dz}\left[\int_{r_o}^{r_c} \rho V_z^2\, (-2\pi r\, dr)\right]\Delta z.$$

Inserting the above expressions into equation 4a, we get cancelling Δz's.

$$4b)\quad -2\pi r_c P_c \frac{dr_c}{dz} - \frac{d}{dz}\left[\int_{r_o}^{r_c} P\, (-2\pi r\, dr)\right] = + \frac{d}{dz}\left[\int_{r_o}^{r_c} \rho V_z^2\, (-2\pi r\, dr)\right]\Delta .$$

Removing one of the V_z's from the integral but not the brackets on the left hand side of the equation, the remaining integral is equal to the flow rate. (eq. 1b) Then

$$4c)\quad \frac{d}{dz}\left[\int_{r_o}^{r_c} P\, (-2\pi r\, dr)\right] = - w_h \frac{dV_z}{dz} - 2\pi r_c P_c \frac{dr_c}{dz}$$

Using assumption #5, we can now find the pressure distribution. Given

$$5a)\quad \frac{\partial P}{\partial r} = \rho \frac{V_\theta^2}{r} = \rho \frac{C(z)^2}{r^3}$$

by integrating this equation we have

$$P = - \frac{\rho\, C(z)^2}{2\, r^2} + A(z).$$

The constant $A(z)$ of the partial r integration being a funtion of z. Since at all z, $r = r_c$, $P = P_c$, $A(z)$ may be determined. The final expression for the pressure distribution is

5b) $$P - P_c = \frac{\rho C(z)^2}{2}\left[\frac{1}{r_c^2} - \frac{1}{r^2}\right].$$

Reinserting this expression into equation 4c and remembering that $r_c = r_c(z)$ and is held constant during the r integration, we get

$$\frac{d}{dz}\left\{\left[P_c + \frac{\rho C(z)^2}{2 r_c^2}\right](\pi r_o^2 - \pi r_c^2) + \pi \rho C(z)^2 \ln\frac{r_c}{r_o}\right\} = -w_h \frac{dV_z}{dz} - 2\pi r_c P_c \frac{dr_c}{dz} .$$

Differentiating this expression and inserting eq. 1d eliminating $\frac{dV_z}{dz}$, we obtain

$$\left[\frac{2\pi r_c w_h^2}{\rho(\pi r_o^2 - \pi r_c^2)^2} - \frac{\pi r_o^2 \rho C(z)^2}{r_c^3} + \frac{\pi \rho C(z)^2}{r_c}\right]\frac{dr_c}{dz} + \frac{dC(z)}{dz}\left[\frac{\pi r_o^2 \rho C(z)}{r_c^2} - \pi \rho C(z) + 2\pi \rho C(z) \ln\frac{r_c}{r_o}\right] = 0 .$$

Inserting eq. 3b to eliminate $\frac{dC(z)}{dz}$ and defining the substitution

6) $$\lambda_z = 1 + \frac{\pi f \rho C_o}{4 w_h} z$$

so that

$$C(z) = \frac{C_o}{\lambda_z} , \quad \frac{dr_c}{dz} = \frac{\pi f \rho C_o}{4 w_h}\frac{dr_c}{d\lambda_z} ,$$

we get

$$\frac{dr_c}{d\lambda_z}\left[\frac{2\pi r_c w_h^2}{\rho(\pi r_o^2 - \pi r_c^2)^2} - \frac{\pi \rho C_o^2 r_o^2}{r_c^3 \lambda_z^2} + \frac{\pi \rho C_o^2}{r_c \lambda_z^2}\right] =$$

$$= - \frac{1}{\lambda_z^3} \left[\frac{\pi \rho r_o^2}{r_c^2} - \pi \rho + 2\pi \rho \, \mathrm{In} \frac{r_c}{r_o} \right] .$$

Rewriting this equation in a different form we have,

$$7) \quad \frac{d\lambda_z}{dz} = \frac{\left[\frac{\pi \rho c_o^2}{r_c} - \frac{\pi \rho c_o^2 r_o^2}{r_c^3} \right] \lambda_z + \left[\frac{2\pi r_c w_h^2}{\rho (\pi r_o^2 - \pi r_c^2)^2} \right] \lambda_z^3}{c_o^2 \left[\frac{\rho (\pi r_o^2 - \pi r_c^2)}{r_c^2} + 2\pi \rho \, \mathrm{In} \frac{r_c}{r_o} \right]}$$

which may be recognized as a Bernoulli differential equation. Accordingly substituting (7)

$$U = \frac{1}{\lambda_z^2} \quad \text{so that} \quad \frac{d\lambda_z}{dr_c} = - \frac{\lambda_z^3}{2} \frac{dU}{dr_c}$$

we have

$$7b) \quad \frac{dU}{dr_c} + \frac{2 \left[\frac{\pi \rho}{r_c} - \frac{\pi \rho r_o^2}{r_c^3} \right] U}{\left[\frac{\rho (\pi r_o^2 - \pi r_c^2)}{r_c^2} + 2\pi \rho \, \mathrm{In} \frac{r_c}{r_o} \right]} = \frac{4\pi r_c \left[- \frac{w_h^2}{\rho (\pi r_o^2 - \pi r_c^2)^2} \right]}{c_o^2 \left[\frac{\rho (\pi r_o^2 - \pi r_c^2)}{r_c^2} + 2\pi \rho \, \mathrm{In} \frac{r_c}{r_o} \right]} .$$

The general form of this equation is

$$8a) \quad \frac{dU}{dr_c} + a_1(r_c) \, U = h(r_c) .$$

If

$$8b) \quad U = \frac{1}{Q} \frac{dQ}{dr_c}$$

may be satsified the general solution of eq. 8a is given as

$$8c)\quad U = \frac{1}{Q}\int Q\, h\, dr_c + \frac{A}{Q}, \qquad (8)$$

where A is an arbitrary constant.

Fortunately in eq.7b the numerator is the exact differential of the denominator, so that eq. 8b. is satsified when

$$8d)\quad Q = \left[\frac{\rho(\pi r_o^2 - \pi r_c^2)}{r_c^2} + 2\pi\rho \ln\frac{r_c}{r_o}\right].$$

Inserting this expression into eq. 8c which conviently cancells the denominator of $h(r_c)$ and integrating, we get

$$9a)\quad U = \frac{\left[A - \dfrac{2\, w_h^2}{\rho C_o(\pi r_o^2 - \pi r_c^2)}\right]}{\left[\dfrac{\rho(\pi r_o^2 - \pi r_c^2)}{r_c^2} + 2\pi\rho \ln\dfrac{r_c}{r_o}\right]}.$$

Equation 9a may be rewritten in dimensionless form by writing the equation in terms of the groups $\frac{r_c}{r_o}$,

$$9b)\quad \lambda_{r_o} = \frac{\pi\rho C_o\, r_o}{4\, w_h},$$

and λ_z. The final solution of the flow pattern is then found to be,

$$10)\quad \frac{\lambda_z^2}{\lambda_{r_o}^2} = \frac{8\left[\left(1 - \dfrac{r_o^2}{r_c^2}\right) - \ln\left(\dfrac{r_c^2}{r_o^2}\right)\right]}{\dfrac{1}{\left(1 - \dfrac{r_c^2}{r_o^2}\right)} + A}.$$

Determination of A

The solution for the flow pattern , eq. 10, is however not as yet complete since neither of the boundary conditions $z = o$, $r_c = r_o$ or $z = \infty$, $r_c = 0$ yield a finite value for the constant A.

One method of determining the constant is to apply Bernoulli's equation at the beginning of the pipe, where an average value of the head is taken.

This condition could be concievably realized if the flow were introduced evenly through a peripheral slit in the wall at the pipe entrance. (See bottom of Fig. 8) If the slit is Δz wide, then in this region there is no wall friction and thus the head can be taken as constant over this small Δz.

This implies that all variations in z are approximately zero over an interval of axial distance, which in the limit can be taken to approach zero.

Bernoulli's equation for an incompressible fluid and a horizontal pipe is

11a) $$\frac{P}{\rho} + \frac{V_\theta^2}{2} + \frac{V_z^2}{2} = gH \quad . \qquad (5)$$

Denoting the initial boundary core radius at the beginning of the pipe by r_i , then at $z = 0$, $V_\theta = \frac{C_o}{r}$ from eq. 3c., $P = P_c + \frac{\rho C_o^2}{2}\left[\frac{1}{r_i^2} - \frac{1}{r^2}\right]$ modifying

eq. 5b and $Vz = \frac{w_h}{\rho(\pi r_o^2 - \pi r_i^2)}$ is obtained from eq. 1c. Inserting the above expressions into eq. 11a , we have after simplification

11b) $$\frac{P_c}{\rho} + \frac{C_o^2}{2 r_i^2} + \frac{w_h^2}{2 \rho^2 (\pi r_o^2 - \pi r_i^2)^2} = gH \ .$$

Since we have assumed that for a short distance near the pipe entrance, all variations in z are neglible and H = constant , we may set $\frac{dH}{d r_c} = 0$.

Performing the differentiation and simplifing we can solve for w_h as

12a) $$w_h = \frac{\pi \rho r_o C_o}{\sqrt{2}} \frac{\left[1 - \left(\frac{r_i}{r_o}\right)^2\right]^{\frac{3}{2}}}{\left(\frac{r_i}{r_o}\right)^2} \ .$$

This can be written in dimensionless form by collecting a λ_{r_o} group. The equation then becomes,

12b) $$\frac{1}{\lambda_{r_o}} = \frac{2\sqrt{2}\left[1 - \left(\frac{r_i}{r_o}\right)^2\right]^{\frac{3}{2}}}{\left(\frac{r_i^2}{r_o^2}\right)}$$

Combining eq. 10 and 12b at z = 0 , where $r_c = r_i$ we may now determine **A** algebracially as

$$13)\quad A = \frac{\left[-\frac{r_i^4}{r_o} \ln \frac{r_i^2}{r_o^2} + \frac{r_i^2}{r_o^2} - 1 \right]}{\left(1 - \frac{r_i^2}{r_o^2}\right)^3}$$

Equations 12b and 13 in combination with equation 10, is the complete solution of the initial problem, and gives curves of the boundary radius r_c or $\frac{r_c}{r_o}$ versus distance down the pipe z or λ_z. The geometrical and fluid constants of the solution are contained in the variable constant λ_{r_o}.

Assuming a knowledge of the physical constants in the system, λ_{r_o} is calculated. This allows the initial core radius ratio to be determined from eq. 12b. This value is then used to determine A in eq. 13, which may be inserted in eq. 10 to give the boundary curve.

In Table 1 in the appendix, values of the above parameters necessary for obtaining any desired curves of r_c versus z for different flow inlet condition are computed and listed.

Discussion of the Results of Part I

A typical solution of the above equations reveals that there are two possible modes of hot air flow down the pipe. An example of the solutions obtainable is shown in Fig. 6a.

One solution which curves away from the wall toward the centerline of the pipe corresponds to an overall decrease in the tangential and axial velocity, as the flow proceeds down the pipe.

A second solution which curves toward the wall, away from the pipe centerline, corresponds to a flow situation where the tangential velocity, while having exactly the same value along the wall as the previous case , now has a much reduced value at the larger core radius of the second case. This means that much of the energy contained in the tangential velocity in the first instance is now used to increase the axial velocity along the wall.

The limiting value of core radius in the second case corresponds to the condition where all of the whirl energy of the flow has been converted into a maximum axial velocity while still allowing passage of all the fluid as required by the continuity equation.

Since no consideration of frictional shear stresses in the axial direction was taken into account in the above solution, at some point down the pipe this layer

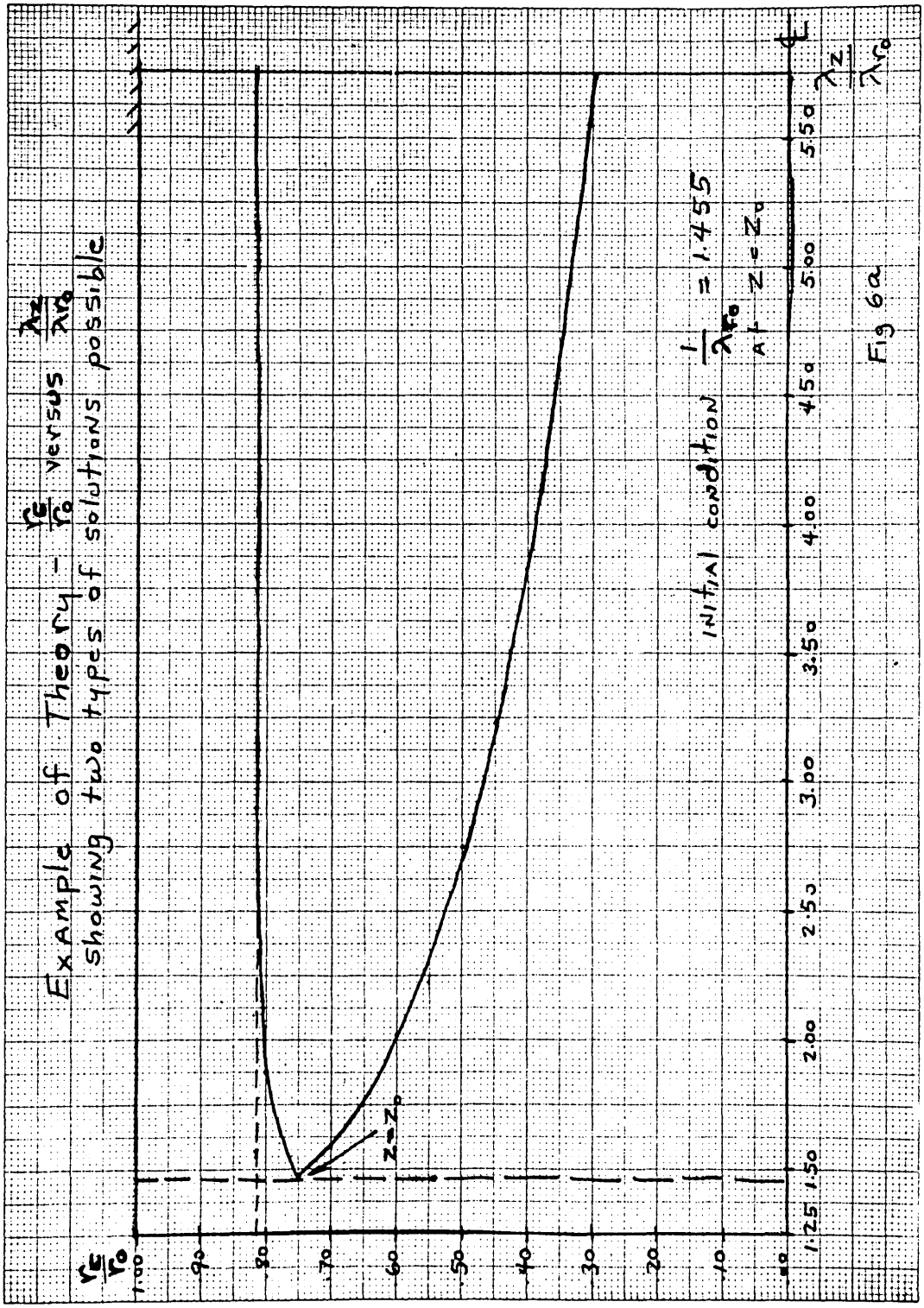
Example of Theory - $\frac{r_E}{r_0}$ versus $\frac{\lambda_z}{\lambda_{r_0}}$
showing two types of solutions possible
$\frac{r_E}{r_0}$
1.00
.90
.80
.70
.60
.50
.40
.30
.20
.10
.00
1.25
1.50
2.00
2.50
3.00
3.50
4.00
4.50
5.00
5.50
$\frac{\lambda_z}{\lambda_{r_0}}$
$z = z_0$
INITIAL condition $\frac{1}{\lambda_{r_0}} = 1.455$ AT $z = z_0$

Fig 6a

would probably experience a hydraulic jump when the critical Reynolds number for air was reached.[16]

Both types of solutions, especially the second one which seems curious, were observed visually by my thesis advisor Prof. J. L. Smith during his doctoral investigation of a cyclone seperator. The model he used to approximate this seperator was very similar to the one[4] outlined above. The flow conditions were such that the approximation of incompressible flow was very nearly true.

Comparison of Model with Data of Reed

The following comparison will show the nature of of the velocity, pressure and streamline profiles as derived theoretically and their deficiencies when compared with actual data. This data is taken from G. A. Reed's Masters thesis performed at M.I.T. in 1947.[9]

Reed measured pressure and temperature profiles inside a Hilsch tube of 2.06" diameter and used one tangentially mounted inlet nozzle of $\frac{3"}{8}$ diameter. One of his runs is reproduced in Fig. 5 .

For this particular run,

P_s = 95 psia $T_s = 560^{\circ}R$ $\rho_s = .460$ lb_m/ft^3 = .452

$$w = \frac{.532\, A^{*}\, P_s}{\sqrt{T_s}} = .235 \text{ lb}_m/\text{ sec.} \quad (6)$$

$$w_h = w(1 - \epsilon) = .128 \text{ lb}_m/\text{ sec}$$

Taking the boundary line of constant pressure to be 14 psig , then $\rho_{avg.}$ may be found by assuming an adiabatic pipe.

$$\rho_{avg.} = \rho_s \left(\frac{P_c}{P_s}\right)^{\frac{1}{k}} = .196 \text{ lb}_m/\text{ ft}^3$$

Since

$$T^{*} = .833 T_s \quad (6) = 466^{o}R$$

and

$$V^{*} = 49 \sqrt{T^{*}} \quad (6) = 1060 \text{ ft/sec} .$$

Then

$$C_o = V^{*}\, r_o = 90.8 \text{ ft}^2/\text{sec}$$

and

$$\lambda_{r_o} = \frac{\pi \rho C_o\, r_o}{4\, w_h} = 11.30 .$$

This determines $\frac{r_i}{r_o}$ in eq. 12b and consequently A in eq. 13 . This parameters were computed to be $\frac{r_i}{r_o} = .953$ and A = - 15.76.

We may use a point on Reed's 14 psig curve to determine a value of f by matching this point on the curve, since

$$\lambda_z = 1 + \frac{\pi f \rho C_o}{4\, w_h} z = 1 + 132\, f\, z .$$

From Reed's data the psig line begins at $z = \frac{1}{3}$ ft. $r_c = .610"$ and $\frac{r_c}{r_o} = .594$.

At this point we then have using eq. 10

$$\left(\frac{1 + 132\, f\, z}{11.30}\right)^2 = \frac{8\left\{\left[1 - \frac{1}{(.594)^2}\right] + \ln \frac{1}{(.594)^2}\right\}}{\frac{1}{1 - (.594)^2} - 15.76}.$$

Solving this equation gives a value $f = .292$, which is 10 times larger than a good average value of $f = .03$. (17)

Knowing A, eq. 10 may now be used to calculate $\frac{\lambda_z}{\lambda_{r_o}}$ versus z .

Other lines of constant pressure may be found by using eq. 5b.

$$P - P_c = \frac{25.1}{\lambda_z^2\, r_c^2}\left[1 - \left(\frac{r_c}{r_o}\right)^2\right]$$

knowing λ_z versus r_c .

The computations indicated above were carried out and are presented in Fig. 6b. As a furthur comparison additional curves were calculated for a friction factor one tenth of the value gotten above.

When the two graphs (Fig 5 and Fig. 6b) are compared it will be noted that there is very little variation in pressure in the theoretical case as compared to the actual example, although there is a general resemblance in the shape of the constant pressure curves.

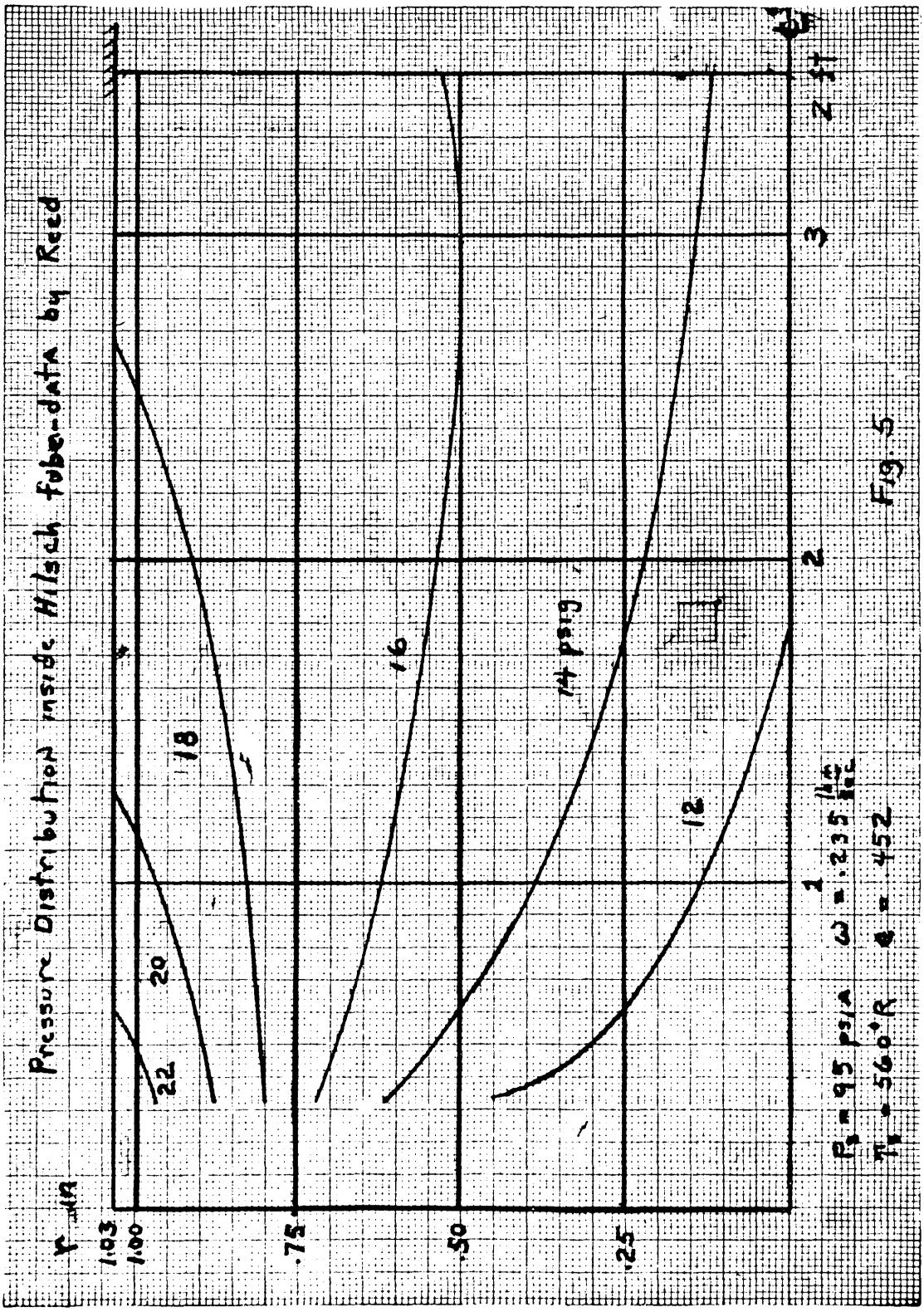
Pressure Distribution inside Hilsch tube-data by Reed
r/R
1.03
1.00
.75
.50
.25
0
1
2
3
4
z ft
22
20
18
16
14 psig
12
P_s = 95 psia ω = .235 lbm/sec
T_s = 560°R Φ = .452

Fig 5

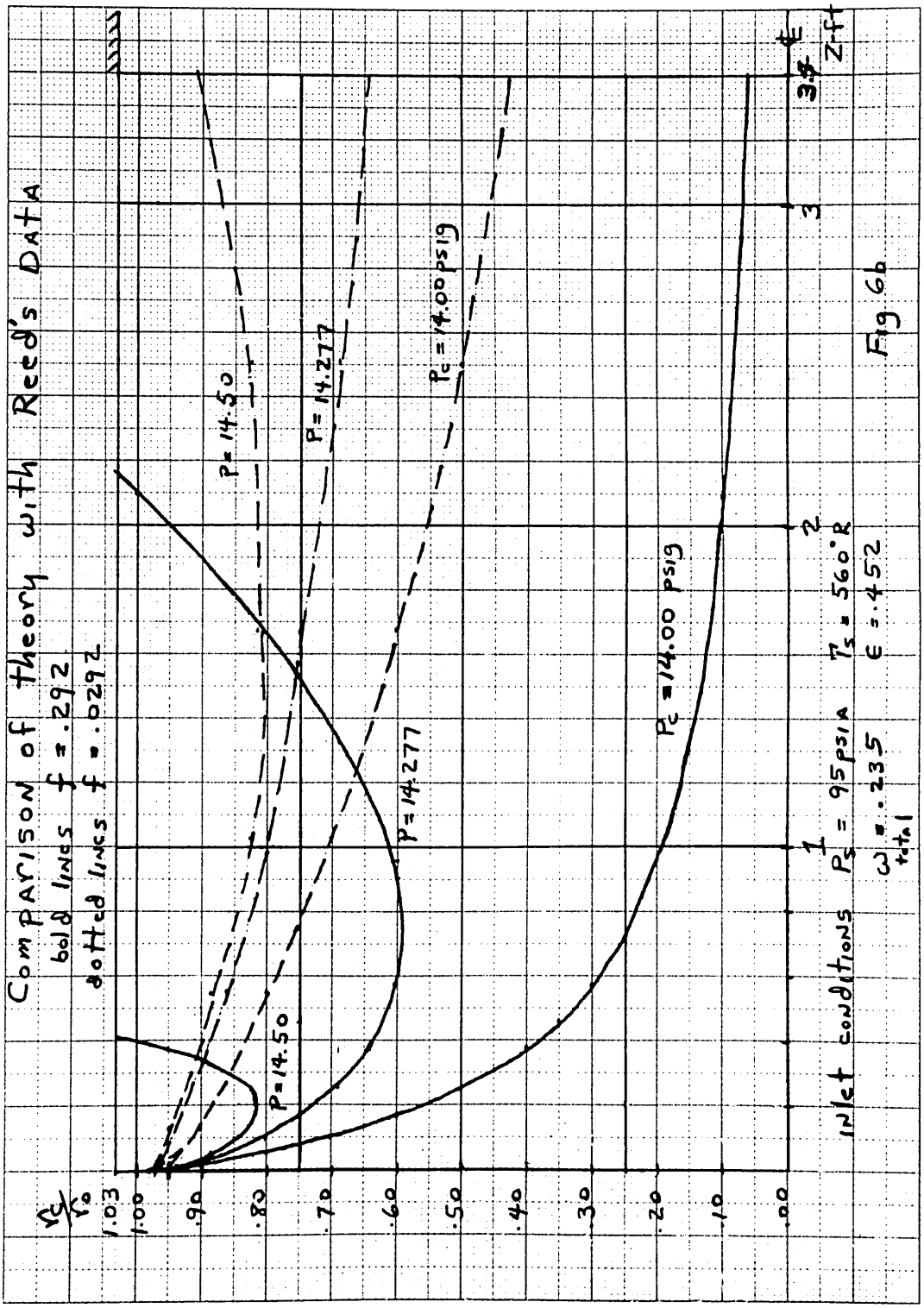
Comparison of theory with Reed's Data
bold lines f = .292
dotted lines f = .0292
$\frac{P_s}{P_0}$
1.03
1.00
.90
.80
.70
.60
.50
.40
.30
.20
.10
.00
P = 14.50
P = 14.277
P = 14.277
P = 14.50
P_c = 14.00 psig
P_c = 14.00 psig
1
2
3
3.5
Z-ft
Inlet conditions P_s = 95 psia T_s = 560°R ϵ = .452
ω_{t+t} = .235

Fig 6b

What seems logically to be the main fault with the theory is that it assumes an incompressible fluid. This is of course not accurate when dealing with pressures measured in atmospheres. The next part of the analysis deals with the above fault.

Part II

Method of Obtaining a Compressible Solution

The solution obtained in Part I can be modified to incorporate compressibility. One immediate object of such a solution would be to obtain the tangential velocity distribution. By then applying the steady flow energy equation to the Hilsch tube the average cold core temperature could be determined. At the present time however the following analysis seems to indicate that to obtain this distribution would require at least a complicated series solution and possibly numerical integration.

The previous assumptions are all retained except that:

#2' The density is allowed to vary adiabatically as

$$\rho = \rho_c \left(\frac{P}{P_c}\right)^{\frac{1}{k}} .$$

#3' The definition of shear stress must be slightly modified to account for variation of density along the wall

$$\tau_o = \frac{f \rho_o V_\theta^2}{8} .$$

From the previous assumption #5 together with assumption #2' leads to expressions for the pressure

and density in the fluid which can be readily found by integration. The constant of integration is eliminated as was previously done in eq. 5b, using the assumption of a constant boundary pressure and density.

The final results are

$$16a)\quad P = P_c \left\{ 1 + \frac{(k-1)\rho_c\, C(z)^2}{2\,k\,P_c} \left[\frac{1}{r_c^2} - \frac{1}{r^2} \right] \right\}^{\frac{k}{k-1}}$$

$$16b)\quad \rho = \rho_c \left\{ 1 + \frac{(k-1)\rho_c\, C(z)^2}{2\,k\,P_c} \left[\frac{1}{r_c^2} - \frac{1}{r^2} \right] \right\}^{\frac{1}{k-1}}$$

These may be writeen

$$16c)\quad P = P_c \left[M(z) - \frac{S(z)}{r^2} \right]^{\frac{k}{k-1}}$$

$$16d)\quad \rho = \rho_c \left[M(z) - \frac{S(z)}{r^2} \right]^{\frac{k}{k-1}}$$

where

$$S(z) = \frac{(k-1)\,C(z)^2 \rho_c}{2\,k\,P_c} \quad \text{and} \quad M(z) = 1 + \frac{S(z)}{r_c^2}$$

The continuity equation is now written as

$$17a)\quad \frac{d}{dz} \left[\int_{r_o}^{r_c} \rho(r,z)\, V_z\, (-2\pi r\, dr) \right] = 0$$

or alternatively

$$17b)\quad w_h = \int_{r_o}^{r_c} \rho(r,z)\, V_z (-2\pi r\, dr) = V_z \int_{r_o}^{r_c} \rho(r,z)(-2\pi r dr)$$

The angular momentum equation is as previously slightly modifying eq. 2b

$$18a)\quad 2\pi r_o^2 \tau_o = -\frac{d}{dz}\left[\int_{r_o}^{r_c} \rho(r,z)\, C(z)\, V_z(-2\pi r\, dr)\right].$$

Removing C(z) from the integral in eq. 18a but not from the brackets, the remaining integral is equal to w_h, so that

$$18b)\quad 2\pi r_o^2 \tau_o = -w_h \frac{dC(z)}{dz}\ .$$

Inserting assumption #2' into eq. 18b) we get finally

$$18c)\quad \frac{dC(z)}{dz} = -\frac{\pi f\, C(z)^2}{4\, w_h}\rho(z,r_o)$$

The axial momentum equation is as previously , eq.4b

$$19a)\ \frac{d}{dz}\left[\int_{r_o}^{r_c} P(-2\pi r\, dr)\right] = -\frac{d}{dz}\left[\int_{r_o}^{r_c} \rho(r,z) V_z^2(-2\pi r\, dr)\right] - 2\pi r_c P_c \frac{dr_c}{dz}$$

Removing V_z from beneath the integral on the right side and substituting w_h from eq. 17b for the resulting integral we have

$$19b)\quad \frac{d}{dz}\left[\int_{r_o}^{r_c} P(r,z)(-2\pi r\, dr)\right] = -w_h \frac{dV_z}{dz} - 2\pi r_c P_c \frac{dr_c}{dz}\ .$$

The last term of the right side may be eliminated by using the following integral theorum

$$20)\quad \frac{d}{dz}\int_{r_o}^{r_c} g(r,z)\,dr = \int_{r_o}^{r_c}\frac{\partial g(r,z)}{\partial z}dr + g(r_c,z)\frac{dr_c}{dz} - g(r_o,z)\frac{dr_o}{dz} \qquad (8)$$

The last term on the right side is zero since r_o is constant. Applying this to eq. 19b we find

$$\int_{r_o}^{r_c}\frac{\partial P(r,z)}{\partial z}(-2\pi r\,dr) + P(r_c,z)(-2\pi r_c)\frac{dr_c}{dz} = -w_h\frac{dV_z}{dz} - 2\pi r_c P_c\frac{dr_c}{dz}\,.$$

Since $P(r_c,z) = P_c$, this simplifies to

$$21)\quad \int_{r_o}^{r_c}\frac{\partial P(r,z)}{\partial z}(-2\pi r\,dr) = -w_h\frac{dVz}{dz}$$

In order to remove $\frac{dV_z}{dz}$ from eq. 21 we can use the continuity equation (eq.17a). First removing V_z from under the integral in 17a and carrying through the z differentiation we have

$$0 = \frac{dV_z}{dz}\left[\int_{r_o}^{r_c}\rho(r,z)(-2\pi r\,dr)\right] + V_z\frac{d}{dz}\left[\int_{r_o}^{r_c}\rho\,(r,z)(-2\pi r\,dr)\right]$$

Applying the integral relation, eq.20 to the second integral in the above equation there results

$$0 = \frac{dV_z}{dz}\left[\int_{r_o}^{r_c}\rho(r,z)(-2\pi r\,dr)\right] + V_z\left[\int_{r_o}^{r_c}\frac{\partial\rho(r,z)}{\partial z}(-2\pi r\,dr)\right] + V_z\rho(r_c,z)(-2\pi r_c)\,.$$

Inserting $\rho(r_c,z) = \rho_c$ and eq. 17b and solving for $\frac{dV_z}{dz}$ we get

$$22)\quad \frac{dV_z}{dz} = -\frac{V_z^2}{w_h}\left[\int_{r_o}^{r_c} \frac{\partial \rho(r,z)}{\partial z}(-2\pi r\, dr) - 2\pi r_c \rho_c\right]$$

The term $2\pi r_c \rho_c$ being present since it has been previously assumed that no fluid crosses the boundary from the rotational to the irrotational region. Inserting eq. 22 into eq. 21, we have the final result,

$$23)\quad \int_{r_o}^{r_c} \frac{\partial P(r,z)}{\partial z}(-2\pi r\, dr) = V_z^2\left[\int_{r_o}^{r_c} \frac{\partial \rho(r,z)}{\partial z}(-2\pi r\, dr) - 2\pi r_c \rho_c\right]$$

The expressions for P and ρ eq. 16c and 16d may now be differentiated with respect to z and inserted in the integrals in eq. 23. Integrating these over r and substituting for V_z from eq. 17b as well as eliminating $\frac{dC(z)}{dz}$ from the result by using eq. 18c , there will result a function of the form

$$h_1\left[\frac{dr_c}{dz},\ r_c\ ,\ C(z)\right] = 0$$

This expression coupled with eq. 18c which is of the form

$$h_2\left[\frac{dC(z)}{dz},\ r_c\ ,\ C(z)\right] = 0$$

should be adequate for a solution.

Part III

Introduction

In looking over the data of various other experimentors who have studied the Hilsch tube (Ref. 9 to 14), it will be noticed that although the pressure at the nozzle exit is high, the pressure along the wall 90 or 180 degrees around the pipe in the nozzle exit plane has dropped a considerable amount. A pressure tap at the wall will read 35 to 80 per-cent of the nozzle throat pressure. The higher pressure Hilsch tubes having the greatest losses.

This is apparently due not only to expansion of the entering gas inward toward the centerline, but axially down the pipe as well.

It was felt that if this pressure loss or part of it could be utilized to increase the velocity of the air entering the chamber above a Mach number of one, then better performance might be expected.

In Fig 7 some previous data is plotted and shows roughly the nature of the pressure loss. Taking an example; if the air has an initial stagnation pressure of 190 psia , then the throat pressure in a converging nozzle would be 100 psia. By introducing this gas directly into the pipe we would suffer 65% losses and the wall pressure would be 35 psia.

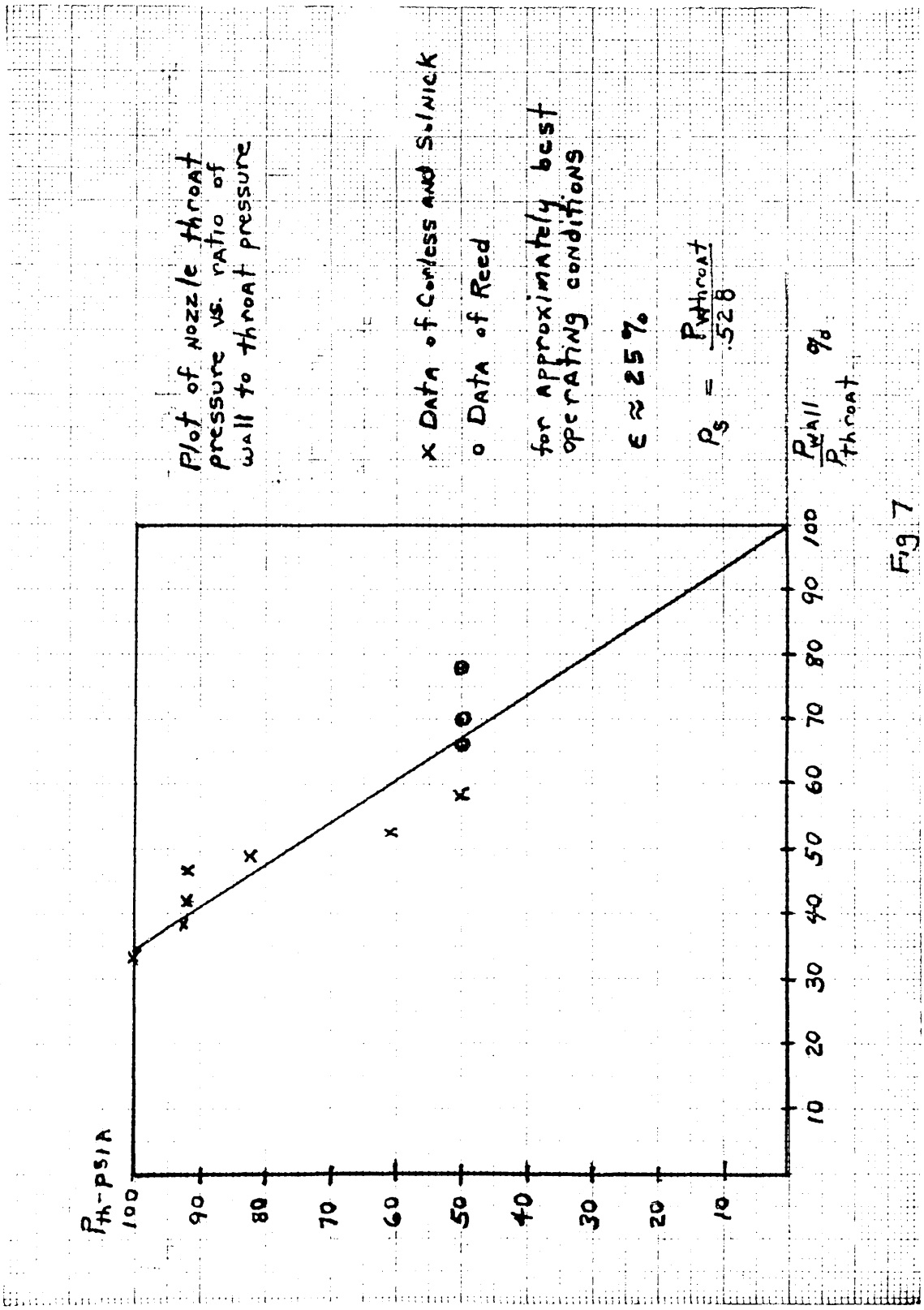
Plot of nozzle throat pressure vs. ratio of wall to throat pressure
x Data of Comess and Silnick
o Data of Reed
for approximately best operating conditions
ε ≈ 25%
$P_s = \frac{P_{wthroat}}{.528}$
P_{th}-PSIA
100
90
80
70
60
50
40
30
20
10
10 20 30 40 50 60 70 80 90 100
$\frac{P_{wall}}{P_{throat}}$ %

Fig 7

In order to utilize some of this pressure loss we could for example introduce the gas through a vortex chamber attachment shown at the bottom of Fig.8 and allow the flow to accelerate as it moved inwardly around the chamber to a higher tangential velocity and lower pressure. By dropping the pressure of the gas leaving the acceleration chamber to 50 psia, the gas entering the pipe would now only suffer 30% losses, and we would still have a wall pressure of 35 psia while gaining 50 psia worth of increase in the tangential velocity.

This pressure loss seems to be a probable explanation for the observed fact that higher pressure devices, although reaching lower cold temperatures, are less efficient.

This idea of using a vortex chamber to pre-accelerate the flow was tried out experimentally and is discussed in the section on experimental work.

Analysis of a Vortex Pre-Accelerator

The following analysis was carried out in order to get an idea of a design criterian for the chamber.

It was assumed that in the chamber there was a free or irrotational vortex, no friction, and symetry in the tangential and axial directions. The density and pressure were allowed to vary adiabatically.

Writing the continuity and Euler's equations in

polar coordinates and introducing the above assumptions, the equations simplify to:[6]

Continuity,

$$24a)\quad \rho\left(\frac{V_r}{r} + \frac{\partial V_r}{\partial r}\right) + V_r\frac{\partial \rho}{\partial r} = 0$$

Tangential Direction,

$$25a)\quad V_r\frac{\partial V_\theta}{\partial r} + \frac{V_r}{r}V_\theta = 0$$

Radial Direction,

$$26)\quad V_r\frac{\partial V_r}{\partial r} - \frac{V_\theta^2}{r} = -\frac{1}{\rho}\frac{\partial P}{\partial r}$$

The continuity equation may be rewritten as

$$\frac{\partial}{\partial r}(\rho V_r r) = 0$$

and gives upon integration

$$24b)\quad w = 2\pi r \rho V_r \Delta z$$

The equation in the tangential direction may be immediately integrated to give the result

$$25b)\quad V_\theta = \frac{C_1}{r}$$

where $C_1 = \dfrac{V_{\text{inlet nozzle}}}{r_1}$

By this substituting this expression for V_θ and the adiabatic gas law

27) $\rho = \rho_1 \left(\frac{P}{P_1}\right)^{\frac{1}{k}}$

into eq. 26 we have

$$V_r \frac{\partial V_r}{\partial r} - \frac{C_1^2}{r^3} = - \frac{1}{\rho_1}\left(\frac{P_1}{P}\right)^{\frac{1}{k}} \frac{\partial P}{\partial r} \quad .$$

Multiplying through by ∂r and integrating, we find

$$\frac{V_r^2}{2} + \frac{C_1^2}{2r^2} = - \frac{k\, P_1^{\frac{1}{k}}}{\rho_1 (k-1)} P^{\frac{k-1}{k}} + B$$

The initial conditions $\frac{V_r^2}{2} + \frac{C_1^2}{2r^2} = \frac{V_1^2}{2}$ When $P = P_1$, are used to determine B.

The equation becomes after simplification

$$28a) \quad \frac{P}{P_1} = \left[1 + \frac{k-1}{2kRT_1}\left(V_1^2 - V_r^2 - \frac{C_1^2}{r^2}\right)\right]^{\frac{k}{k-1}}$$

Using eq. 27 as well as the perfect gas law, to obtain the relation between the pressure and density ratios, and substituting in the expression for V_r from eq. 24b , we get an expression for the density ratio as

$$28b) \quad \frac{\rho}{\rho_1} = \left[1 + \frac{k-1}{2kRT_1}\left(V_1^2 - \frac{C_1^2}{r^2} - \frac{w^2}{4\pi^2 r^2 \Delta z^2 \rho^2}\right)\right]^{\frac{1}{k-1}} .$$

The equation for the temperature is found in a similar fashion to be

$$28c) \quad \frac{T}{T_1} = \left[1 + \frac{k-1}{2kRT_1}\left(V_1^2 - V_r^2 - \frac{C_1^2}{r^2}\right)\right]$$

Eq. 28b may be modified by substitutiong in the continuity equation $w_1 = \rho_1 V_1 A_1$ and the definition of the Mach number

$$29) \quad M_1 \doteq \frac{V_1}{\sqrt{kRT_1}} \quad (6)$$

to give after simplification

$$\left(\frac{\rho}{\rho_1}\right)^{k-1} = 1 + \frac{k-1}{2} M_1^2 \left[\left(1 - \frac{r_1^2}{r^2}\right) - \frac{\rho_1^2}{\rho^2} \frac{A_1}{4\pi^2 r^2 \Delta z^2}\right]$$

Multiplying the above equation by $\left(\frac{\rho}{\rho_1}\right)^2$ and rewriting it in terms of the temperature ratio, then replacing T by T_o, r by r_o the final result arrived at will be

$$30) \left(\frac{T_o}{T_1}\right)^{\frac{k+1}{k-1}} - \left(\frac{T_o}{T_1}\right)^{\frac{2}{k-1}} \left[1 + \frac{k-1}{2} M_1^2 \left(1 - \frac{r_1^2}{r_o^2}\right)\right] + \frac{k-1}{2} M_1^2 \left(\frac{A_1^2}{2\pi r_o \Delta z}\right)^2 = 0$$

An additional useful result may be gotten from the definition of the Mach number (eq.29) and the tangential velocity equation (25b), $C_o = V_{\theta_o} r_o = V_{\theta_1} r_1$

$$M_1 = \frac{V_1}{\sqrt{kRT_1}} = \frac{V_{\theta_o} r_o}{\sqrt{kRT_1}} \cdot \frac{\sqrt{kRT_o}}{\sqrt{kRT_o}}$$

giving the result

$$31) \quad \frac{M_{\theta_o}}{M_1} = \frac{r_1}{r_o} \sqrt{\frac{T_1}{T_o}}$$

It is also handy to know that $\left(\frac{r_1}{r_o}\right)_{max}$ occurs when the radial Mach number is one.

At this point

$$32)\left(\frac{T_o}{T_1}\right)_{\text{for } \frac{r_1}{r_o} \max} = \frac{1 + \frac{k-1}{2} M_1^2 \left(1 - \frac{r_1^2}{r_o^2}\right)}{\frac{k+1}{2}} ,$$

which is easily gotten from eq. 28c.

Putting the above expression into eq.30 , $\left(\frac{r_1}{r_o}\right)$max is found to occur when

$$33)\left(\frac{r_1^2}{r_o^2}\right) = 1 + \frac{1 + \frac{k-1}{2}\left[\frac{M_1 A_1}{2\pi r_o \Delta z}\right]^{\frac{2(k-1)}{k+1}}}{\frac{k-1}{2} M_1^2}$$

In figure 8 equation 30 is solved and plotted with the aid of eqs. 31, 32, and33 as $\frac{T_o}{T_1}$ and $\frac{P_o}{P_1}$ versus $\frac{r_1}{r_o}$ for an inlet air Mach number of 1; k was taken as 1.4 .

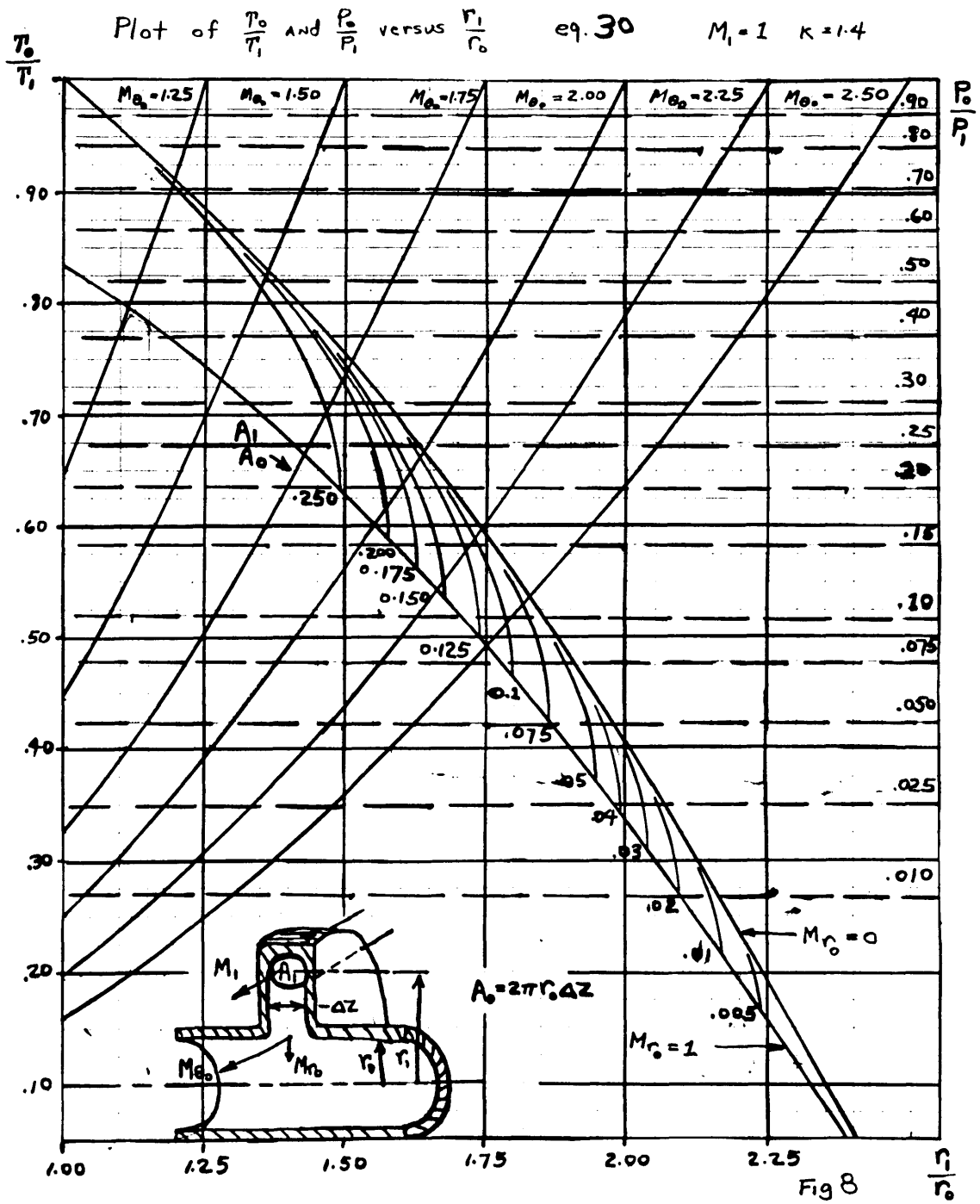
Plot of $\frac{T_o}{T_i}$ AND $\frac{P_o}{P_i}$ versus $\frac{r_i}{r_o}$ eq. 30 $M_i = 1$ $K = 1.4$
$\frac{T_o}{T_i}$
$\frac{P_o}{P_i}$
$M_{\theta_o} = 1.25$
$M_{\theta_o} = 1.50$
$M_{\theta_o} = 1.75$
$M_{\theta_o} = 2.00$
$M_{\theta_o} = 2.25$
$M_{\theta_o} = 2.50$
$\frac{A_i}{A_o}$
.250
.200
0.175
0.150
0.125
0.1
.075
.05
.04
.03
.02
.01
.005
$M_{r_o} = 0$
$M_{r_o} = 1$
M_i
A_i
Δz
M_{θ_o}
M_{r_o}
r_o
r_i
$A_o = 2\pi r_o \Delta z$
1.00
1.25
1.50
1.75
2.00
2.25
$\frac{r_i}{r_o}$

Fig 8

Experimental Work

Object

one of the objects of the experiments undertaken, was to test, by comparitive data, the idea of adding a vortex chamber pre-accelerating attachment, in an attempt to improve the efficiency of the Hilsch tube.

A second object of the experimentation was to examine the effect of placing various size flow restricting circular weirs at the end of the hot pipe in an attempt to increase the performance of the refrigerator.

This second idea originally arose from erroneous theoretical considerations which indicated that by placing a weir of the proper size on the pipe, it might be possible to decrease the length to diameter ratio from an experimentally observed optimum of 50 to a lesser value while still maintaining the same level of performance. The analysis was wrong but since an effect, even though apparently negative, was observed; data and discussion of the idea is included in this thesis for future reference.

Procedure

A simple experimental setup was constructed from partially available equiptment in order to test the above

ideas. The vortex chamber used had a $\frac{3"}{4}$ inside diameter and was fed by two $\frac{1"}{8}$ diameter converging nozzles, placed symetrically.

Thermocouples were placed directly in the hot and cold air flows in order to measure the temperatures of the air streams. Two pressure taps were placed $1\frac{1"}{2}$ from both ends of the hot pipe. A weir and needle valve device was built and installed on the end of the hot pipe and an orifice flow meter was placed on the cold end of the pipe. Additional details of construction are shown in Figs. 13 and 14 in the appendix.

The total flow was estimated at a known P_s and T_s by completely closing up the hot end and blowing all the air through the flow meter on the cold end, after which it was only necessary to measure the cold flow. The flow measurement data is listed in Table 2 in the appendix.

Using a hot pipe of length to diameter ratio of 33 with an inside diameter of $\frac{3"}{4}$, three weir to pipe radius ratios $\frac{r_w}{r_o}$ of $1, \frac{2}{3}, \frac{1}{2}$ were tried out with a $\frac{3"}{16}$ cold flow diaphragm in runs 1, 2, and 3 and a $\frac{7"}{32}$ cold diaphragm in runs 4, 5, and 6. The plots of this data are shown in Figs. 9 and 10 .

The $\frac{3"}{4}$ pipe was then removed and a .546" inside diameter pipe with the same length to diameter ratio,

was inserted in its place. A cold diaphragm geometrically similar to that used in runs 1, 2, and 3 of diameter .136" was then inserted.

This reduced pipe radius now allowed the flow to pre-accelerate in the $\frac{3"}{4}$ diameter vortex chamber before entering the hot pipe.

For this vortex chamber the pipe radius ratio of $\frac{.750}{.546} = 1.37$, the tangential Mach number of the flow entering the pipe may be read off Fig. 8 and is approximately 1.50 since the vortex chamber was still wide enough that the radial Mach number was approximately zero.

For this $\frac{r_1}{r_o}$ ratio, the pressure ratio is seen to be $\frac{P_o}{P_1} = .50$. With an initial P_s of 170 psia the pressure in the air inlet nozzle throat is then $P_1 = .528\ P_s$ (6) = 90 psia, so that theoretically P_o should be 45 psia.

This value is 8 psia higher then the data of Fig. 7 indicates.

With this smaller pipe, weir to pipe radius ratios of 1, $\frac{2}{3}$, and $\frac{1}{2}$ were again tried out in runs 7, 8, and 9.

The plot of this data is shown in Fig. 11 .

A comparison of runs 1 and 7 , showing the effect of preaccelerating the flow with no weir is plotted in Fig. 12 .

Table 3 in the appendix lists all data taken and calculations performed.

Discussion of Experimental Results

The effect of placing various weirs at the end of the hot pipe without the pre-accelerator attached to the pipe, is seen in Figs. 9 and 10 to be observable but apparently detrimental, although only three weir sizes were used. Using intermediate weir sizes, especially between the ratios of $\frac{r_w}{r_o} = 1$ and $\frac{r_w}{r_o} = \frac{2}{3}$ might concievably give improved or equal performance by increasing the $\frac{L}{D}$ ratio in this case from 33 to the experimental optimum.

The effect of pre-accelerating the flow before it entered the pipe did improve the performance of the Hilsch tube. The temperature of the cold air was found to be 20°F colder for the same flow rates, then a geometrically similar tube with no pre-acceleration, as may be seen in Fig. 12 .

With both types of tubes it was noted that with the smaller size weirs, the flow resistance became so great, as to raise the pressure inside the pipe to a high value. This set a minimum amount of flow which could be passed out the cold end. These smaller weirs thus restricted performance by forcing the ratio of cold air flow to total flow above the value for optimum operation.

For this setup ϵ was approximately 10%, a figure about half the value found by other experimentors to be an optimum. This was attributed to the lack of a sharp

edged cold orifice. In its place, a relatively long (1 inch) piece of threaded bar with the proper size hole drilled through it was used.

This idea was verified by placing a sharp edged cold orifice in the device. For best performance ϵ was then found to increase to 16% , as is indicated in run #10, tabled in the appendix.

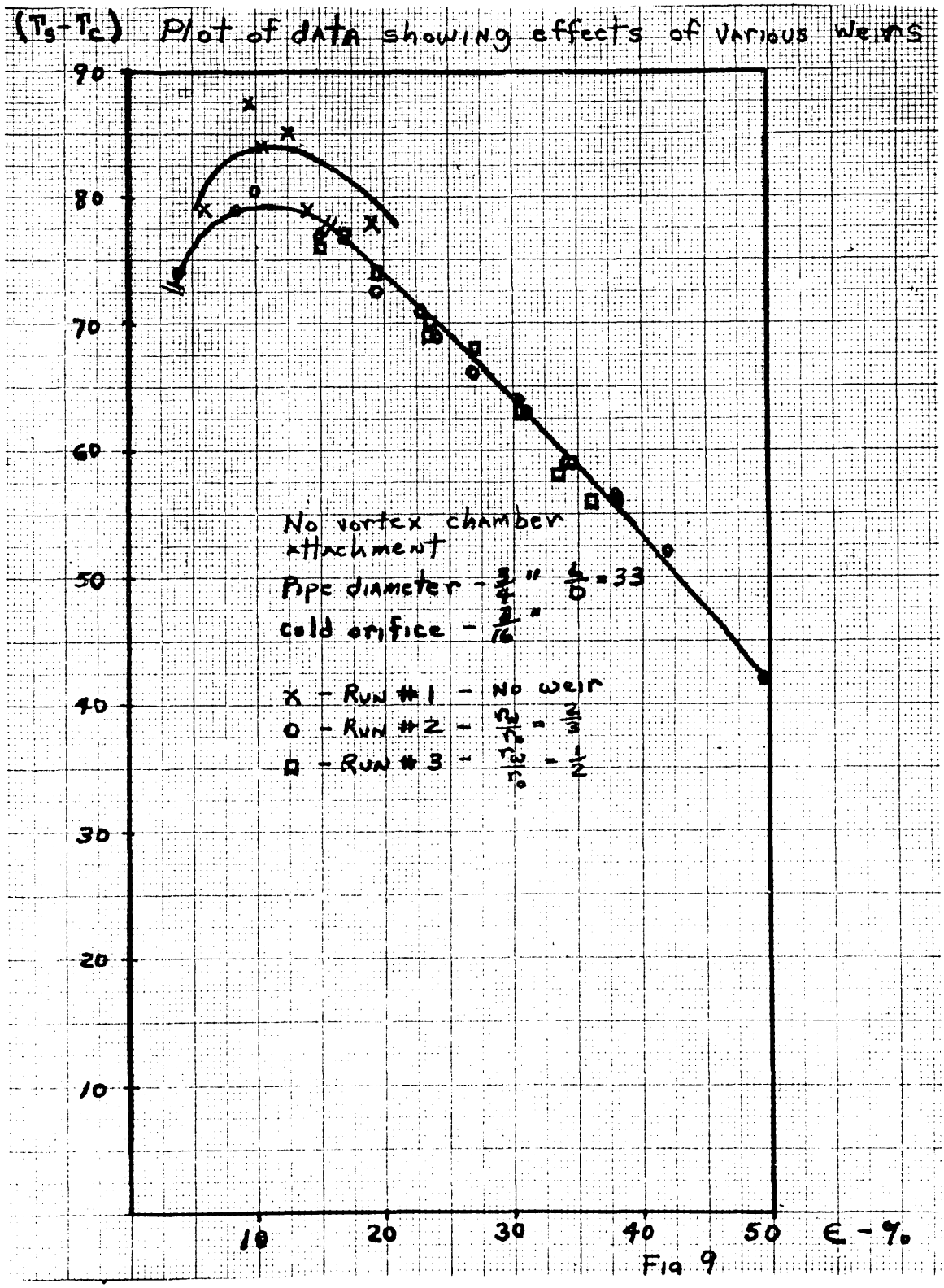
$(T_s - T_c)$ Plot of data showing effects of various weirs
90
80
70
60
50
40
30
20
10
10
20
30
40
50
ϵ - %
No vortex chamber attachment
Pipe diameter - $\frac{3}{4}$" $\frac{L}{D}$ = 33
Cold orifice - $\frac{3}{16}$"
x - Run #1 - No weir
o - Run #2 - $\frac{3/4}{3/4} = \frac{3}{3}$
□ - Run #3 - $\frac{3/4}{1.5/8} = \frac{1}{2}$

Fig 9

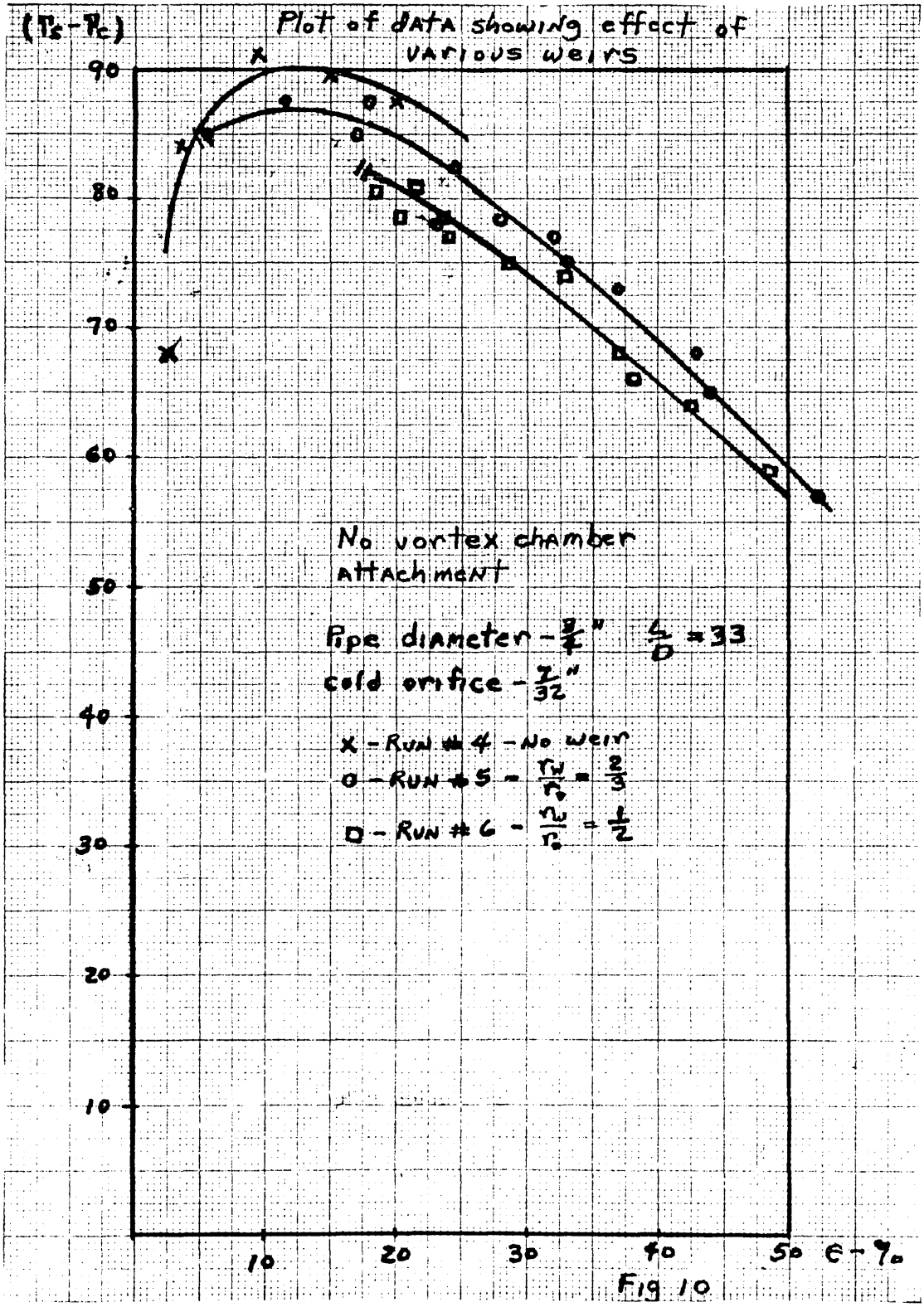
$(P_s - P_c)$
Plot of data showing effect of various weirs
90
80
70
60
50
40
30
20
10
No vortex chamber attachment
Pipe diameter - $\frac{3}{4}$"
$\frac{L}{D} = 33$
cold orifice - $\frac{7}{32}$"
X - Run # 4 - No weir
o - Run # 5 - $\frac{r_w}{r_p} = \frac{2}{3}$
□ - Run # 6 - $\frac{r_w}{r_p} = \frac{1}{2}$
10
20
30
40
50
ϵ - %

Fig 10

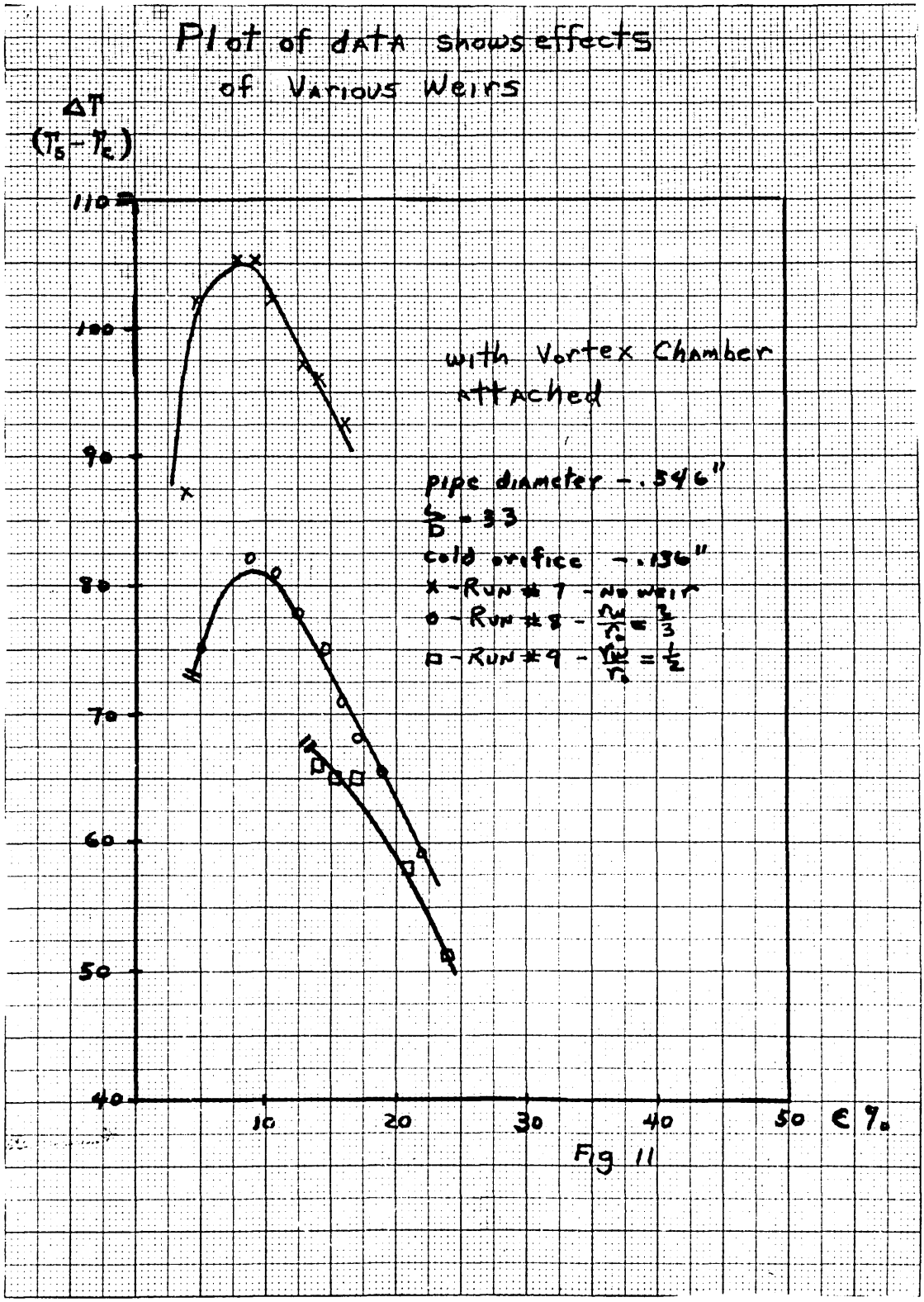
Plot of data shows effects of Various Weirs
ΔT (T5 - T2)
110
100
90
80
70
60
50
40
10
20
30
40
50
€ %
with Vortex Chamber attached
pipe diameter - .546"
L/D = 3
cold orifice - .136"
x - Run # 7 - No weir
o - Run # 8 - rw/r2 = 2/3
□ - Run # 9 - rw/r2 = 1/2

Fig 11

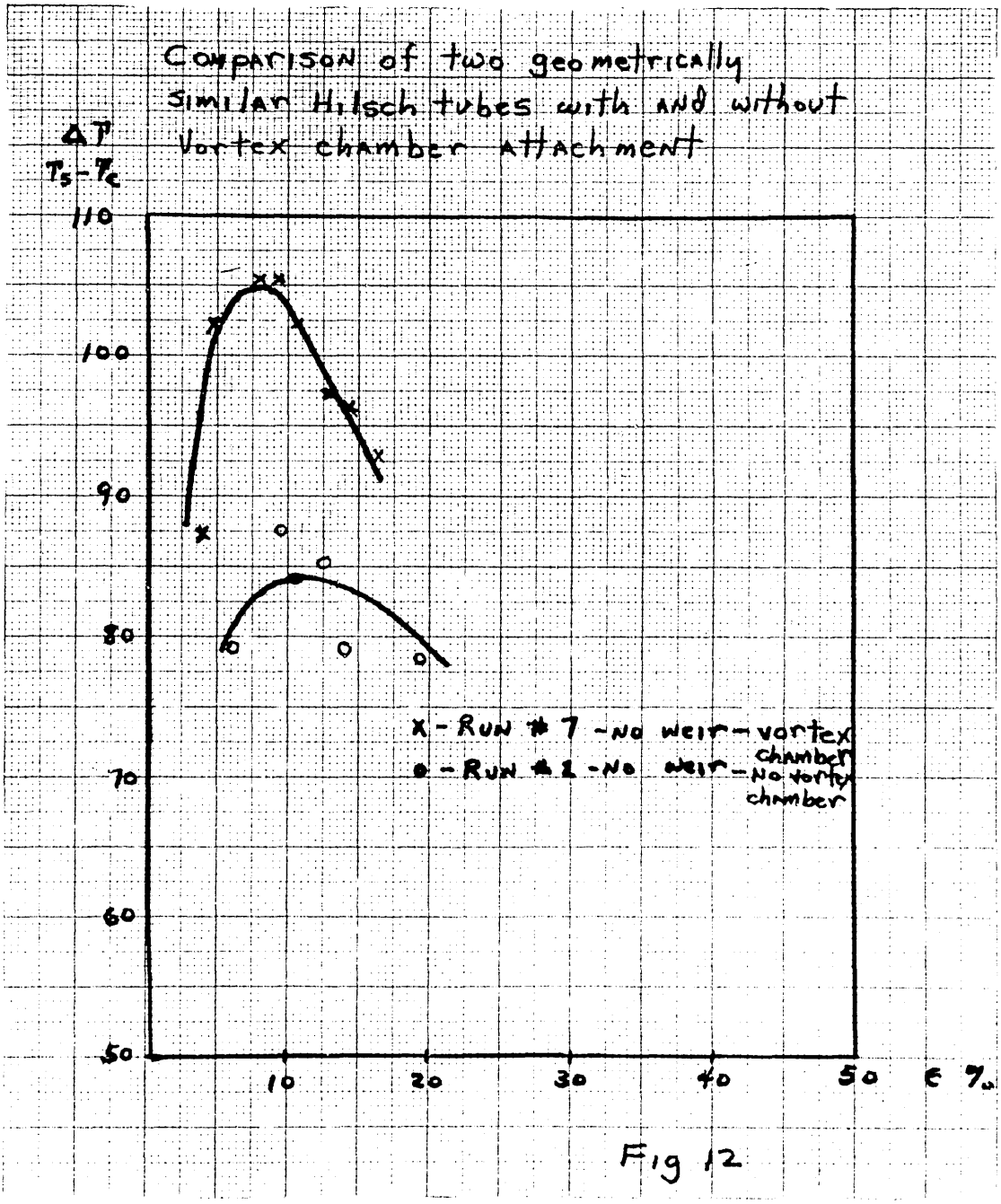
Comparison of two geometrically similar Hilsch tubes with and without vortex chamber attachment
ΔT
$T_s - T_c$
110
100
90
80
70
60
50
10
20
30
40
50
ε %
x - Run # 7 - No weir - vortex chamber
o - Run # 2 - No weir - No vortex chamber

Fig 12

Bibliography

1. Scientific American, Nov. 1958 , P. 145.
2. Hilsch, R. ,"The Use of the Expansion of Gases in A Centrifugal Field as a Cooling Process" , Review of Scientific Instruments, Vol. 18 , No. 2, Feb. 1947.
3. Lay, J. E., "An Experimental and Analytical Study of Vortex-Flow Temperature Seperation by Superposition of Spiral and Axial Flow", ASME paper 58 - A - 90 .
4. Smith, J.L., "An Experimental and Analytic Study of the Vortex in Cyclone Seperators" Phd Thesis Course II M.I.T., Jan.1959 .
5. Hunsaker, J.C. and Rightmire, B.G., "Engineering Applications of Fluid Mechanics", Mc Graw Hill Book Co., 1947.
6. Shapiro, A.H., "The Dynamics and Thermodynamics of Compressible Fluid Flow", Vol.1 , Roland Press Co. 1954.
7. Martin W.T., and Reissner E., "Elementary Differential Equations", Addison-Wesley Publishing Co. Inc.1956.
8. Hildebrand, F.B.,"Advanced Calculus for Engineers", Prentice-Hall Inc,1949.

9. Reed G.A., "Vortex Tube Refrigeration", M. S. thesis Course XVI M.I.T.,1947.

10. Corless, R.J.Jr.,andSolnick,R.L.,"Experimental Investigation of Vortex Refrigeration",B.S.thesis Course II M.I.T., 1947.

11. Fattah, M.N. and Sweeny A.N.,"Experimental Investigation of Centrifugal Refrigeration", B.S.Thesis Course II M.I.T.,1947.

12. Haddox,R. , Hunter, J.W. and Plunkett, W.H. "Experimental Study of Centrifugal Refrigeration" B.S. thesis Course II M.I.T., 1947.

13. Hunter,J.W., and Bruce H. Mayer ,"Centrifugal Refrigeration" B.S. thesis Course II M.I.T. 1947.

14. Nickerson, R.J.,"Vortex Flow of a Compressible Fluid", B.S. thesis Course II, M.I.T. 1949

15. Wilson,W.A.,"Foster,E.L.,"Experimental Heat-Power Engineering", M.E. Dept. M.I.T. 1956.

16. Rouse,H. and Howe,J.W., "Basic Mechanics of Fluids", John Wiley and Sons,Inc. 1953. P.162.

17. Giedt,W.H.,"Principles of Engineering Heat Transfer", D. Van Nostrand Co. Inc. 1957, P.107.

Appendix

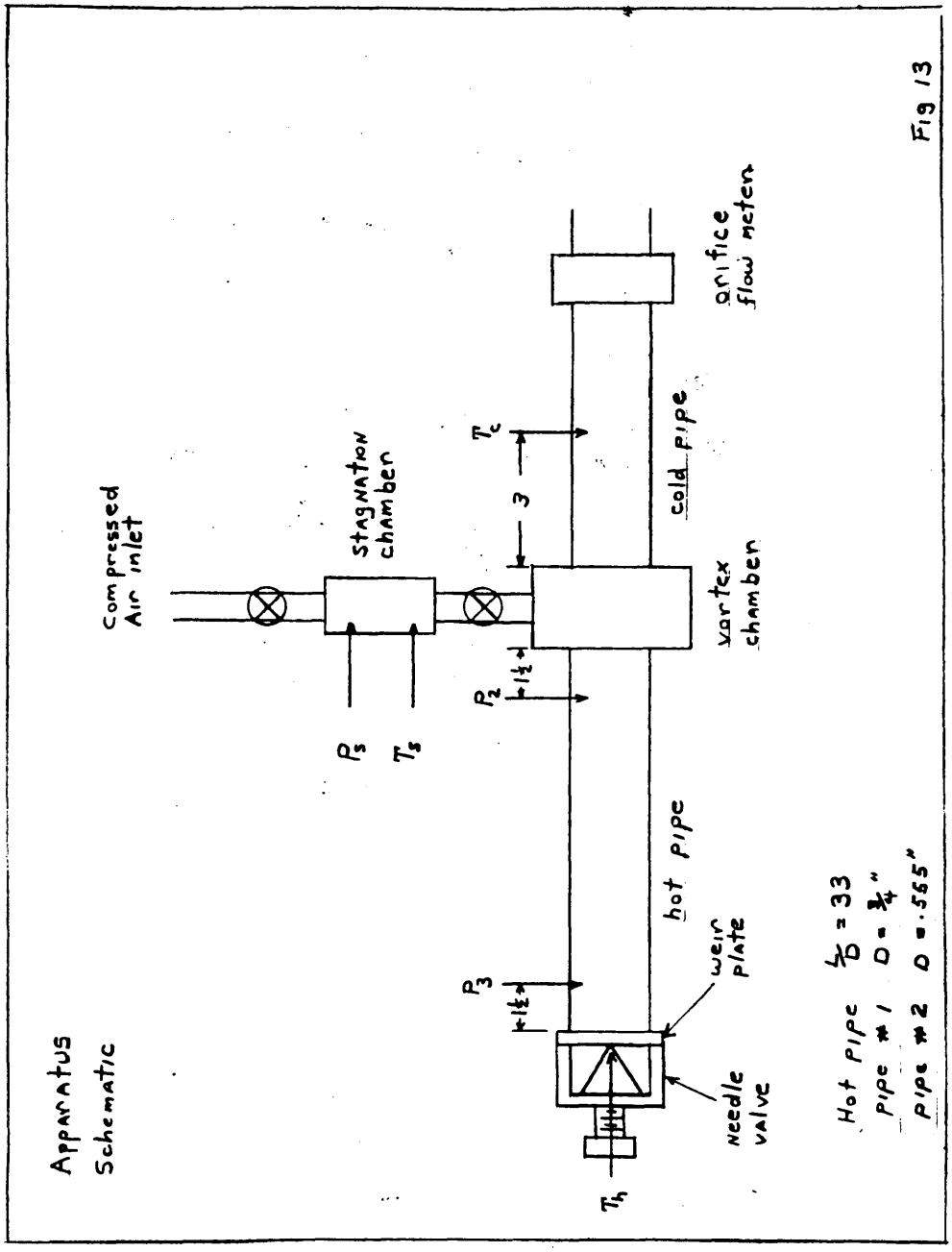
Apparatus
Schematic
Compressed
Air inlet
stagnation
chamber
P_s
T_s
P_2
1½"
T_c
3
vortex
chamber
cold pipe
orifice
flow meter
P_3
1½"
hot pipe
weir
plate
needle
valve
T_h
Hot pipe $\frac{L}{D} = 33$
pipe #1 D = ¾"
pipe #2 D = .555"

Fig 13

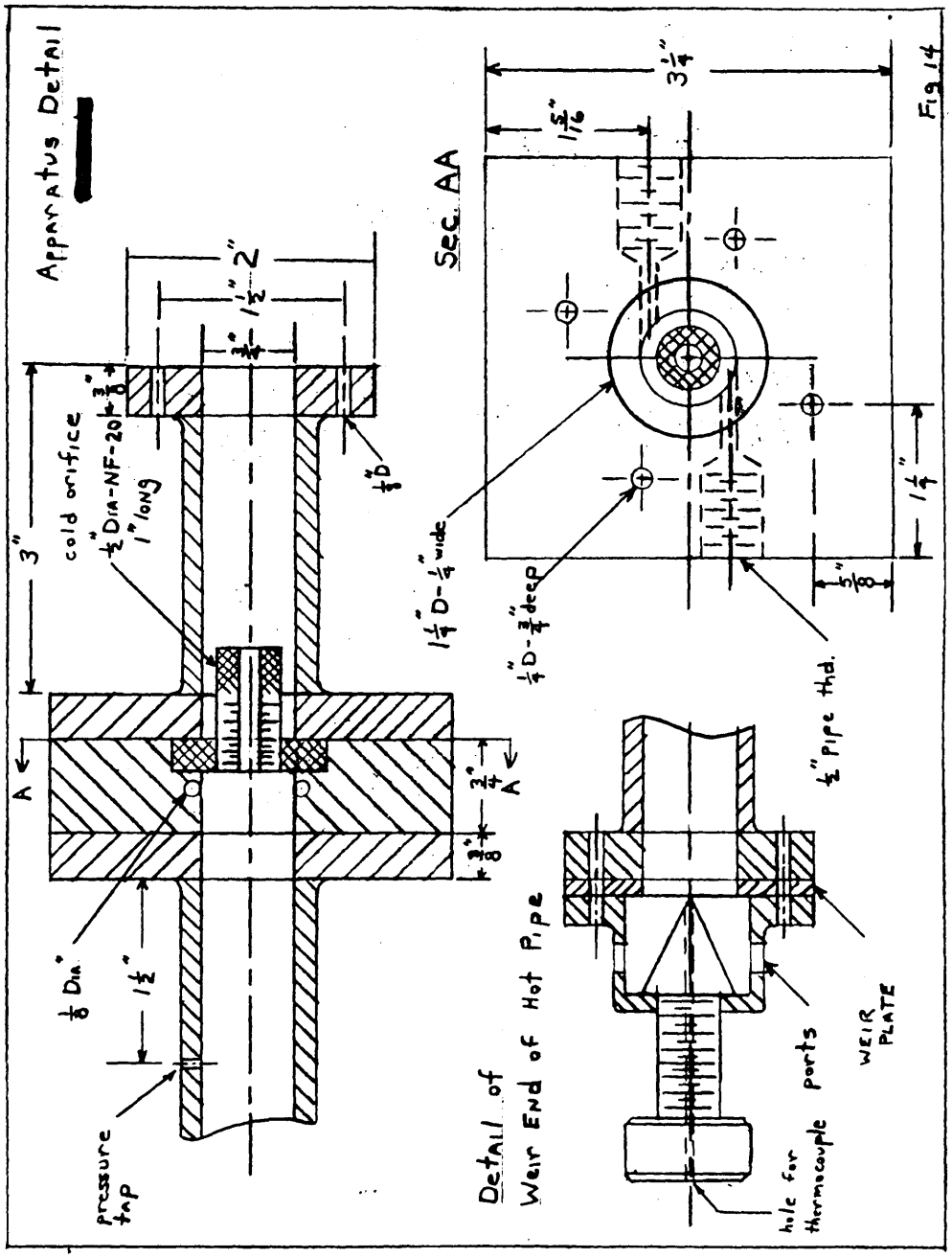
Apparatus Detail
Sec. AA
Detail of
Weir End of Hot Pipe
cold orifice
pressure tap
hole for thermocouple
WEIR PLATE
Fig. 14

Table 1a

$\frac{r_s}{r_0}$	$\frac{1}{\lambda r_0}$	A
1.00	0	$-\infty$
.95	.0955	-15.016
.90	.290	-7.52
.85	.571	-5.14
.80	.954	-3.800
.75	1.455	-3.047
.70	2.105	-2.552
.65	2.94	-2.199
.60	4.02	-1.938
.55	5.44	-1.736
.50	7.35	-1.572
.45	9.95	-1.443
.40	13.60	-1.3390
.35	18.95	-1.2523
.30	27.3	-1.1817
.25	41.2	-1.1235
.20	66.5	-1.07917
.15	121.5	-1.0442
.10	278.	-1.01985
.05	1128.	-1.00517
.00	∞	-1.0000

$$\frac{1}{\lambda r_0} = 2\sqrt{2}\,\frac{\left[1-\left(\frac{r_s}{r_0}\right)^2\right]^{\frac{3}{2}}}{\left(\frac{r_s}{r_0}\right)^2}$$

$$A = \frac{\left[-\left(\frac{r_s}{r_0}\right)^4 \ln\left(\frac{r_s}{r_0}\right)^2 + \left(\frac{r_s}{r_0}\right)^2 - 1\right]}{\left(1-\frac{r_s^2}{r_0^2}\right)^3}$$

Procedure

Knowing physical constants determine λr_0 which gives $\frac{r_s}{r_0}$ and A.

Using table 1b along with A gives various points on the curves.

Table 1b

$\frac{r_c}{r_0}$	$8\left[\left(1-\frac{r_0^2}{r_c^2}\right)-\ln\left(\frac{r_c}{r_0}\right)^2\right]$	$\frac{1}{1-\frac{r_c^2}{r_0^2}}$
1.00		∞
.95	-.04344	10.2564
.90	-.1908	5.26316
.85	-.4728	3.6036
.80	-.9298	2.77778
.75	-1.6176	2.2857
.70	-2.62	1.96078
.65	-4.04	1.7315
.60	-6.05	1.56250
.55	-8.93	1.4336
.50	-12.9	1.3333
.45	-18.7	1.2539
.40	-27.3	1.190476
.35	-40.5	1.1395
.30	-61.6	1.098901
.25	-96.8	1.0666
.20	-166	1.041667
.15	-317	1.0229
.10	-755	1.010101
.05	-3140	1.00250
.00	$-\infty$	1.0000

$$\left(\frac{\lambda_z}{\lambda_{r_0}}\right)^2 = \frac{8\left[\left(1-\frac{r_0^2}{r_c^2}\right)-\ln\left(\frac{r_c}{r_0}\right)^2\right]}{\frac{1}{\left(1-\frac{r_c^2}{r_0^2}\right)}+A}$$

Table 2a

Flow measurement data

barometer 30.2 in Hg = 14.85 psia

$$\omega = .668\, A\, K E Y \sqrt{\rho_{x_B} \Delta P} \quad \frac{lbm}{sec} \quad (15)$$

K - empirical - .650

E - expansion factor - neglected

$Y \simeq .675 + .325 \frac{P_A}{P_B}$ for this orifice

$\rho_{x_B} = {}^{lbm}/_{ft^3}$

$\Delta P = P_B - P_A$

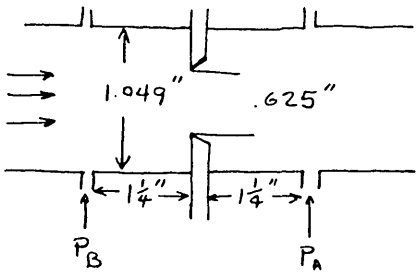

P_s psig	T_s °F	P_{1B} psia	ΔZ in" Hg	P_A psia	P_A/P_B	Y	T_B °R	ω_{actual} lbm/sec	$\omega_{theoritical}$
150	80	16.84	5.125	16.84	.852	.951	526	.0588	.0930
155	80	16.97	5.50	16.97	.840	.948	526.5	.0612	.0958
160	80	17.09	5.8125	17.09	.828	.944	527	.0628	.0985

For this particular orifice

P_B - psia T_B - °R

$$\omega = .153\, Y \sqrt{\frac{P_B}{T_B} \Delta Z_M}$$

ΔZ_M - inches Hg

$$\omega = .0415\, Y \sqrt{\frac{P_B}{T_B} \Delta Z_{H_2O}}$$

ΔZ_{H_2O} - inches H_2O

theoritically

$$\omega = .01305 \frac{P_s}{\sqrt{T_s}} \quad (4)$$

P_s - psia

T_s - °R

Table 3a Data

Run # 1 $\frac{3}{16}$" cold orifice - $\frac{3}{4}$" hot orifice barometer 30.2 in" H_g
P_s - 169.85 psia T_s - 541°R - 81°F $\omega_{total} \cong .0612 \frac{lbm}{sec}$

P_2 psig	P_3 psig	$T_c = T_B$ °F	ΔT $(T_s - T_c)$	Δz inches H_2O	P_B psia	ω_c lbm/sec	ϵ
8.5	3	79	2°	-.45			
11.5	5	78	3°	0	14.85	0	0
14.5	7.5	2	79	.25	14.86	.00371	.0605
16.5	10	-6.5	87.5	.60	14.87	.00581	.0945
19.0	12.5	-3	84	.70	14.87	.00626	.102
21.5	15	-1.5	85.5	1.05	14.89	.00766	.125
26	20	+2	79	1.30	14.90	.00851	.139
30.5	25	+3	78	2.50	14.93	.0117	.191

Run # 2 $\frac{3}{16}$" cold orifice - $\frac{1}{2}$" hot orifice barometer 30.2 in" H_g
P_s - 169.85 psia T_s - 540°R - 80°F $\omega_{total} \cong .0612 \frac{lbm}{sec}$

P_2 psig	P_3 psig	$T_c = T_B$ °F	ΔT $(T_s - T_c)$	Δz inches H_2O	P_B psia	ω_c lbm/sec	ϵ
15	9	6	74	.10	14.85	.00232	.0378
19	12.5	1	79	.50	14.87	.00527	.0862
21.5	15	-.5	80.5	.65	14.87	.00601	.0982
25.5	20	3	77	1.50	14.90	.00913	.149
30.5	25	5	75	2.55	14.94	.0119	.194
35.5	30	9	71	3.50	14.98	.0140	.229
40.5	35	14	66	4.90	15.03	.0164	.268
45.5	40	16	64	6.40	15.08	.0186	.304
50	45	21	59	8.10	15.14	.0208	.340
55	50	24	56	10.3	15.22	.0234	.382
60	55	28	52	12.35	15.30	.0255	.417
69.5	65	38	42	17.55	15.48	.0302	.494
55	50	24	56	10.35	15.22	.0234	.382
50	45	21	59	8.35	15.15	.0211	.345
45.5	40	17	63	6.55	15.09	.0189	.308
35.5	30	11	69	3.95	14.99	.0148	.242
26	20	3	77	1.90	14.92	.0103	.168

Table 3a) DATA

RUN # 3 $\frac{3}{16}$ cold orifice - $\frac{3}{8}$ hot orifice barometer 30.18 in"Hg
P_s - 169.8 PSIA T_s - 546°R - 86°F $\omega_{total} \approx .0612 \frac{lbm}{sec}$

P_2 PSIG	P_3 PSIG	$T_c = T_B$ °F	ΔT $(T_s - T_c)$	ΔZ inches H_2O	P_{13} PSIA	ω_c $\frac{lbm}{sec}$	ϵ
25.5	20	10	76	1.6	14.91	.00932	.152
30.5	25	12	74	2.6	14.94	.0119	.195
36	30	16	70	3.75	14.98	.0143	.234
40.5	35	18	68	5.05	15.03	.0164	.268
45.5	40	23	63	6.55	15.09	.0188	.306
50	45	28	58	7.95	15.14	.0206	.336
55	50	30	56	9.90	15.21	.0220	.359
45.5	40	23	63	6.40	15.08	.0186	.304
36.5	30	17	69	3.75	14.98	.0143	.234
26.0	20	9	77	1.95	14.92	.0103	.168

RUN # 4 $\frac{7}{32}$ cold orifice - $\frac{3}{4}$ hot orifice barometer 30.18 in Hg
P_s - 169.8 PSIA T_s - 544°R - 84°F $\omega_{total} \approx .0612 \frac{lbm}{sec}$

P_2 PSIG	P_3 PSIG	$T_c = T_B$ °F	ΔT $(T_s - T_c)$	ΔZ inches H_2O	P_{13} PSIA	ω_c $\frac{lbm}{sec}$	ϵ
10	3.5	70°	14	-.25			
11.5	5	68	16	0			
14	7.5	7	77	.30	14.81	.00128	.021
17	10	2	82	.75	14.82	.00643	.105
19	12.5	-.5	84.5	1.60	14.86	.00943	.154
21.5	15	+1	83	2.40	14.89	.0116	.190
25.5	20	2	82	3.75	14.94	.0145	.237
21.5	15	-3.5	87.5	2.70	14.90	.0123	.200
19.5	12.5	-5.5	89.5	1.50	14.85	.00922	.151
17	10	-7.5	91.5	.60	14.82	.00581	.095
14	7.5	-.5	84.5	.10	14.80	.00236	.0386
11.5	5.0	16	68	.05	14.80	.00164	.0268

Table 3a Data

RUN # 5 $\frac{7}{32}$ cold orifice - $\frac{1}{2}$ hot orifice barometer 30.18 in Hg
P_s - 169.8 PSIA T_s - 542°R - 82°F $\omega_{total} \approx .0612 \frac{lbm}{sec}$

P_2 PSIG	P_3 PSIG	$T_c = T_B$ °F	ΔT ($T_s - T_c$)	ΔZ inches H_2O	P_B PSIA	ω_c lbm/sec	ϵ
15	10	-3	85	+.20	14.81	.00334	.0546
19	12.5	-5.5	87.5	1.15	14.84	.00805	.131
21	15	-3	85	1.95	14.87	.0104	.171
25.5	20	4	78	3.65	14.93	.0142	.232
30.5	25	3	79	5.25	1499	.0172	.281
35	30	5	77	7.00	15.02	.0197	.322
40.5	35	9	73	9.20	15.13	.0226	.370
45.5	40	14	68	12.45	15.25	.0262	.428
55	50	25	57	20.20	15.53	.0333	.545
46	40	17	65	13.15	15.28	.0270	.442
36	30	7	75	7.40	15.07	.0203	.332
26	20	-.5	82.5	4.00	14.94	.0150	.245
21.5	15	-5.5	87.5	2.20	14.88	.0110	.180

RUN # 6 $\frac{7}{32}$ cold orifice - $\frac{3}{8}$ hot orifice barometer 30.18
P_s - 169.8 PSIA T_s - 538°R - 78°F $\omega_{total} = .0612 \frac{lbm}{sec}$

P_2 PSIG	P_3 PSIG	$T_c = T_B$ °F	ΔT ($T_s - T_c$)	ΔZ inches H_2O	P_B PSIA	ω_c lbm/sec	ϵ
24.5	17.5	-2.5	80.5	2.30	14.88	.0113	.185
26	20	-.5	78.5	2.75	14.90	.0124	.203
30.5	25	1	77	3.95	1494	.0148	.242
35.5	30	4	74	7.30	15.06	.0202	.330
40.5	35	10	68	9.20	15.13	.0226	.369
45.5	40	14	64	12.25	15.24	.0260	.425
50.5	45	19	59	16.00	15.30	.0298	.487
41	35	12	66	9.65	15.15	.0232	.380
31	25	3	75	5.40	14.99	.0174	.285
26	20	-.5	78.5	3.80	14.94	.0145	.237
24.5	17.5	-3	81	3.15	14.91	.0131	.214

Table 3a Data

Run # 7 .136" cold orifice -.546" hot orifice barometer 30" Hg
P_s - 169.70 psia T_s - 551 °R - 91°F $\omega_{total} \simeq .0612 \frac{lbm}{sec}$

P_2 psig	P_3 psig	$T_c = T_B$ °F	ΔT $(T_s - T_c)$	Δz inches H_2O	P_B psia	ω_c $\frac{lbm}{sec}$	ϵ
19	5	88	3	-.0			
24	10	88	3	-.0			
26	12.5	89	2	+.05			
28	15	4	87	+.10	14.70	.00234	.0383
30.5	17.5	-11	102	.15	14.70	.00288	.0470
32.5	20	-18	109	.25	14.71	.00478	.0780
36.5	25	-18	109	.55	14.72	.00562	.0920
41	30	-11	102	.75	14.73	.00650	.106
45.5	35	-6	97	1.15	14.74	.00805	.132
50	40	-5	96	1.30	14.75	.00855	.140
54.5	45	-1.5	92.5	1.75	14.76	.00987	.161
59.5	50	+3	88	2.10	14.78	.0106	.173

Run # 8 .136" cold orifice -.364" hot orifice barometer 30" Hg
P_s - 169.7 psia T_s - 548°R - 88°F ω_{total} - .0612 $\frac{lbm}{sec}$

P_2 psig	P_3 psig	$T_c = T_B$ °F	ΔT $(T_s - T_c)$	Δz inches H_2O	P_B psia	ω_c $\frac{lbm}{sec}$	ϵ
36.5	25	13	75	.20	14.71	.00328	.0498
40	30	6	82	.55	14.72	.00548	.0895
45	35	7	81	.80	14.73	.00660	.108
49.5	40	10	78	1.10	14.74	.00770	.126
54.5	45	13	75	1.45	14.75	.00884	.145
59	50	17	71	1.80	14.76	.00979	.160
63.5	55	20	68	2.05	14.77	.0106	.172
67.5	60	22.5	65.5	2.55	14.79	.0116	.191
76	70	30	58	3.45	14.82	.0134	.219

Table 3a Data

Run # 9 .136 cold orifice -.273 hot orifice barometer 14.7 psia
P_s = 169.7 psia T_s = 548°R - 88°F ω_{total} = .0612 $\frac{lbm}{sec}$

P_2 psig	P_3 psig	$T_c = T_B$ °F	ΔT $(T_s - T_c)$	ΔZ inches H_2O	P_B psia	ω_c lbm/sec	ϵ
55.5	46	22	66	1.35	14.75	.00848	.138
58.5	50	23	65	1.65	14.76	.00934	.153
63	55	23	65	2.05	14.77	.0104	.170
73	65	30	58	3.20	14.81	.0129	.211
81	75	37	51	4.20	14.85	.0147	.240

Run # 10 $\frac{3}{16}$ sharp edged cold orifice -.546 hot orifice
P_s - 169.8 psia T_s - 540°R - 80°F $\omega_{total} \cong .0615 \frac{lbm}{sec}$
barometer 30.2" Hg

P_2 psig	P_3 psig	$T_c = T_B$ °F	ΔT $T_s - T_c$	ΔZ inches H_2O	P_B psia	ω_c lbm/sec	ϵ
15	1	79	1	-.45	14.8		
23.5	10	76	4	0	14.8		
27.5	15	21	59	.10	14.8	.00230	.0376
30	17.5	-1	81	.45	14.81	.00500	.0817
32.5	20	-11	91	1.05	14.84	.00772	.126
35	22.5	-15	95	1.20	14.86	.00830	.136
37	25	-22	102	1.70	14.87	.0100	.1635
39	27.5	-19	99	2.00	14.90	.0108	.176
44	32.5	-15	95	2.80	14.95	.0127	.208
50	40	-7	87	4.30	15.00	.0156	.255
58	50	10	70	6.40	15.03	.0187	.306
67.5	60	22	58	9.85	15.15	.0231	.378

Note: extensive time taken in tabulating this data does not necessarily indicate it is usable for accurate quantitative purposes.